

TRACKING CHANGES IN RESILIENCE AND LEVEL OF COORDINATION IN TERRORIST GROUPS

BY VASANTHAN RAGHAVAN,^{*} AND ALEXANDER G. TARTAKOVSKY[†]

Qualcomm Flarion Technologies^{} and University of Connecticut[†]*

Activity profiles of terrorist groups show frequent spurts and downfalls corresponding to changes in the underlying organizational dynamics. In particular, it is of interest in understanding changes in attributes such as intentions/ideology, tactics/strategies, capabilities/resources, etc., that influence and impact the activity. The goal of this work is the quick detection of such changes and in general, tracking of macroscopic as well as microscopic trends in group dynamics. Prior work in this area are based on parametric approaches and rely on time-series analysis techniques, self-exciting hurdle models (SEHM), or hidden Markov models (HMM). While these approaches detect spurts and downfalls reasonably accurately, they are all based on model learning — a task that is difficult in practice because of the “rare” nature of terrorist attacks from a model learning perspective. In this paper, we pursue an alternate non-parametric approach for spurt detection in activity profiles. Our approach is based on binning the count data of terrorist activity to form observation vectors that can be compared with each other. Motivated by a *majorization theory* framework, these vectors are then transformed via certain functionals and used in spurt classification. While the parametric approaches often result in either a large number of missed detections of real changes or false alarms of unoccurred changes, the proposed approach is shown to result in a small number of missed detections *and* false alarms. Further, the non-parametric nature of the approach makes it attractive for ready applications in a practical context.

1. Introduction. Changes in the organizational dynamics of terrorist groups lead to either spurts or downfalls in their activity profiles. It is of interest in detecting such changes, associating these changes to specific macroscopic changes in group dynamics, and in tracking these dynamics over time. Prior work in this area has primarily been of a parametric nature.

Initial work on monitoring terrorist network activity profiles follows the interrupted time-series framework where the main goal is to study whether certain strategic policy interventions lead to statistically significant reduction in certain types of attacks and/or if different types of attacks act as substitutes for/complements of each other. This is achieved by isolating the time of intervention, fitting (potentially different) threshold vector auto-regression models to the time-series data before and after the intervention is introduced, and inferencing on its efficacy; see, works by Landes (1978); Cauley and Im (1988); Enders and Sandler

AMS 2000 subject classifications: Primary 62P25, 62M99; secondary 62L10, 62G99

Keywords and phrases: Hidden Markov model, terrorism analysis, terrorist groups, changepoint detection, non-parametric approaches, spurt detection, majorization theory

(1993, 2000), for example. In another parametric direction, group-based trajectory analyses are adopted by Dugan, LaFree and Piquero (2005) and LaFree, Morris and Dugan (2010) to identify regional terrorism trends via the use of Cox proportional hazards model or zero-inflated Poisson model. A similar philosophy of identifying common trends across multiple terrorist groups is also adopted by Breiger et al. (2011); Melamed et al. (2012) and Bakker, Raab and Milward (2012).

Two recent approaches in modeling activity profiles have been along the directions of: i) self-exciting hurdle models (SEHM) (Hawkes, 1971; Mohler et al., 2011; Porter and White, 2012) and ii) hidden Markov models (HMM) (Raghavan, Galstyan and Tartakovsky, 2013). While both approaches leverage the sparsity of activity profiles and account for clustering of attacks, they do so via different mechanisms. In the SEHM approach, the hurdle component creates data sparsity by ensuring a pre-specified density of zero counts, while the self-exciting component induces clustering of data. In the HMM approach, an increase or decrease in the attack intensity is attributed to switching between internal states that captures the dynamics of the group’s evolution.

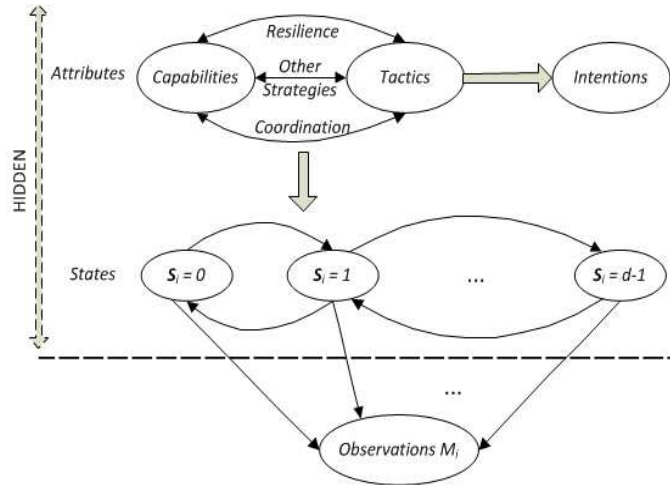


FIG 1. A typical mechanistic model capturing the dynamics of a terrorist group with connections between the underlying attributes, states and observations.

The HMM framework (Raghavan, Galstyan and Tartakovsky, 2013; Raghavan, 2016) provides good explanation/prediction capability of past/future activity across a large set of terrorist groups with different ideological attributes and is thus of main focus in this work. This framework is motivated by a typical mechanistic model proposed by Cragin and Daly (2004) and illustrated in Fig. 1 that captures the complex correlations in time and network structure of the activity profile. Some of the terrorist group attributes capturing the dynamics in this model include its *Intentions*, its *Capabilities*, and the underlying *Tactics* deployed by it to utilize its *Capabilities* in realizing its *Intentions*. Of particular interest in this work are *Tactics* that reflect a strong *Resilience* and/or *Coordination* in the group since they capture counter-terrorism dynamics; see Sec. 2 for precise definitions and works

by Sageman (2004); Cragin and Daly (2004); Santos (2011); Bakker, Raab and Milward (2012); Lindberg (2010); Blomberg, Gaibulloev and Sandler (2011); Breiger et al. (2011); Melamed et al. (2012) for motivations in tracking these particular *Tactics*.

The work by Raghavan, Galstyan and Tartakovsky (2013) bins the activity data into decision interval blocks, leverages the underlying HMM structure, and proposes a state estimation strategy for spurt detection under certain assumptions. While useful, technical difficulties ensured that a complementary view of this strategy where the states are estimated over the entire interval and are then binned into decision interval blocks was not considered by Raghavan, Galstyan and Tartakovsky (2013). We overcome these technical difficulties and provide this missing link in this work. We note that both approaches lead to acceptable inferencing performance on the terrorist group and allow attribution to specific *Tactics* that could have induced a change in the overall activity profile. However, it is unclear if either approach is optimal from an inferencing perspective for the underlying *Tactic*. Further, both approaches suffer from a fundamental issue in that they are retrospective or non-causal (models are first learned over the data followed by inferencing). Thus, such approaches are difficult to implement in practice since terrorist activity data is sparse from a model learning perspective and latencies in model learning could render assumptions on model stability questionable.

Given this backdrop, the major contributions of this work are as follows.

- We propose a non-parametric approach to detect changes in the activity profile and to attribute them to specific changes in the underlying *Tactics* deployed by the group. For this, we develop an application of majorization theory (commonly used as a partial ordering to compare probability vectors) in terrorism analysis. Motivated by a theory of reverse majorization, we build on the partial ordering via the use of certain functionals that serve as a proxy for complete ordering of attack frequency vectors. We then identify a subset of these functionals to capture changes in *Resilience* (or *Coordination*) better and use these associations to track changes in group dynamics.
- We conduct extensive numerical studies with both data generated from the mechanistic model in Fig. 1 as well as real data from the *Fuerzas Armadas Revolucionarias de Colombia* (FARC) terrorist group from Colombia (RDWTI). We show that the proposed non-parametric approach results in both a small number of false alarms declaring changes in *Tactics* when there are none *and* a small number of missed detections of real changes in *Tactics*. On the other hand, the parametric approaches based on the HMM framework either result in low probability of false alarm or low probability of missed detection, but not both.
- These observations suggest that the non-parametric approach provides a suitable compromise not only in terms of its practical utility, but also in terms of performance with real terrorist data.

2. Problem Setup. The observations capturing the dynamics of a terrorist group are multivariate and are of a mixed (categorical, ordinal and interval variables) type, e.g., time and location of attacks, type of ammunition used, (apparent) sub-group of the group in-

volved, intensity and impact of the attacks, etc. In addition, the observations can suffer from impairments such as missing data, mislabeled data, temporal and attributional ambiguity, transcribing errors, etc. We start by developing a temporal model for the activity profile by discarding the categorical and ordinal variables.

2.1. *Temporal Modeling of Activity Profiles.* Let the first and last day of the time-period of interest be denoted as Day 1 and Day N , respectively. Let \mathbf{M}_i denote the number of terrorism incidents on the i th day of observation, $i = 1, \dots, N$. Note that $\mathbf{M}_i \in \{0, 1, 2, \dots\}$ with $\mathbf{M}_i = 0$ corresponding to no terrorist activity on the i th day of observation. Let \mathbf{H}_i denote the history of the group's activity till (and including) day i . That is, $\mathbf{H}_i = \{\mathbf{M}_1, \dots, \mathbf{M}_i\}$, $i = 1, 2, \dots, N$ with $\mathbf{H}_0 \triangleq \emptyset$ (denoting the null set). The temporal point process model is completely specified when $\mathbb{P}(\mathbf{M}_i = r | \mathbf{H}_{i-1})$ is known as a function of \mathbf{H}_{i-1} for all $i = 1, \dots, N$ and $r = 0, 1, 2, \dots$.

With the HMM framework, [Raghavan, Galstyan and Tartakovsky \(2013\)](#) hypothesize that the observations \mathbf{M}_i depend only on certain hidden states \mathbf{S}_i (such as *Intentions*, *Tactics*, or *Capabilities*) in the sense that \mathbf{M}_i is conditionally independent of \mathbf{H}_{i-1} and \mathbf{S}_{i-1} given \mathbf{S}_i . Further, they assume a time-homogenous one-step Markovian evolution for \mathbf{S}_i with a d -state model to capture the dynamics of the group over time. That is, $\mathbf{S}_i \in \{0, 1, \dots, d-1\}$ with each distinct value corresponding to a different level in the underlying attribute of the group. Using these two hypotheses, the temporal point process model can be written as

$$\mathbb{P}(\mathbf{M}_i = r | \mathbf{H}_{i-1}) = \sum_{j=0}^{d-1} \sum_{k=0}^{d-1} \mathbb{P}(\mathbf{M}_i = r | \mathbf{S}_i = j) \cdot \mathbb{P}(\mathbf{S}_i = j, \mathbf{S}_{i-1} = k).$$

The trade-off between accurate modeling of the group's attributes (larger d is better for this goal) versus estimating more model parameters¹ (smaller d is better for this goal) is resolved by [Raghavan, Galstyan and Tartakovsky \(2013\)](#) by focussing on mature terrorist groups (where the *Intentions* attribute remains stable) and by considering a $d = 2$ setting. This trade-off corresponds to a binary quantization of the group's *Tactics* and *Capabilities* into *Active* and *Inactive* states.

For the observations, a simple two-parameter model such as the *hurdle-based geometric* density, defined as,

$$(2.1) \quad \mathbb{P}(\mathbf{M}_i = r | \mathbf{S}_i = j) \triangleq \text{HBG}(\mu_j, \gamma_j) = \begin{cases} 1 - \gamma_j, & r = 0 \\ \gamma_j(1 - \mu_j) \cdot (\mu_j)^{r-1}, & r \geq 1 \end{cases}$$

can be hypothesized. The intuition behind the hurdle-based geometric model is that the terrorist group remains *oblivious* of its past activity and continues to attack with the same *Tactics* as before, as long as its short-term objective is met, provided a certain group resistance/hurdle has been overcome. The special case where there is no group resistance to this aforementioned strategy is obtained by setting $\mu_j = \gamma_j$, resulting in a geometric observation density.

¹The number of model parameters in the HMM framework is $d(d-1+\ell)$ where ℓ is the (common) number of observation density parameters in each state.

2.2. *Underlying Assumptions and Problem Statements.* We make the following assumptions in this work.

Assumption 1: Motivated by the efforts in (Raghavan, Galstyan and Tartakovsky, 2013; Raghavan, 2016), we assume that terrorist activity can be accurately described by a $d = 2$ -state HMM with observations following the hurdle-based geometric density in (2.1). Specifically, let \mathcal{H}_j denote the hypothesis that $\mathbf{S}_i = j$ and the observation model is given as

$$\mathcal{H}_j : \mathbf{M}_i \sim \text{HBG}(\mu_j, \gamma_j), j \in \{0, 1\},$$

with a state transition probability matrix

$$\mathbf{T}(\mathbf{p}_0, \mathbf{p}_1) = \begin{bmatrix} 1 - \mathbf{p}_0 & \mathbf{p}_0 \\ \mathbf{q}_0 & 1 - \mathbf{q}_0 \end{bmatrix}$$

capturing the dynamics of evolution from \mathbf{S}_{i-1} to \mathbf{S}_i .

Assumption 2: With the mechanistic model of Cragin and Daly (2004) as the backdrop, we are primarily interested in two specific types of *Tactics* deployed by the group: Those *Tactics* reflecting i) *Resilience* and ii) a high level of *Coordination* in the group. These *Tactics* are important since they determine the broad outline of counter-terrorism policies and measures sustained by the establishment (see related works by Sageman (2004); Cragin and Daly (2004); Santos (2011); Lindberg (2010); Blomberg, Gaibullov and Sandler (2011); Bakker, Raab and Milward (2012); Breiger et al. (2011); Melamed et al. (2012) for motivations on the focus on these *Tactics*). To be specific, resilience is defined as the ability of the group to sustain terrorist activity over a number of days and this ability reflects the group's capacity to rejuvenate itself from asset (manpower, material, and skill-sets) losses. On the other hand, coordination is defined as the ability of the group to launch multiple attacks over a given time-period and this ability reflects its capacity to coordinate the group's assets necessary for simultaneous action over a wide geography.

Assumption 3: Assuming a stable set of *Intentions* for the group (e.g., mature groups) and with a focus on its *Tactics* and *Capabilities*, the first problem of interest in this work is to quickly arrive at specific/microscopic inferencing decisions on disruptions in the group's activity profile (with typical interest on spurts and downfalls). The second problem of interest is of a broad/macrosopic nature: whether these disruptions could be attributed either to a change in the group's resilience, or a change in the level of coordination between different sub-groups of the group, or both of these attributes.

Assumption 4: Inferencing with $\{\mathbf{M}_i\}$ on a daily basis could lead to a performance mirroring the potential rapid fluctuations in the observations. This is particularly disadvantageous in making global policy decisions on the group. To overcome this problem, we propose inferencing over a $\delta > 1$ day *disjoint* time-window. For this, we decompose the time-period of interest into disjoint time-windows, Δ_n , $n = 1, 2, \dots, K$, where $\Delta_n = \{(n-1)\delta + 1, \dots, n\delta\}$ and $K = \lfloor N/\delta \rfloor$. The appropriate choice of δ is determined by the group dynamics and the timelines for inferencing decisions with typical choices being 7 or 14 days corresponding to a weekly or a bi-weekly decision process.

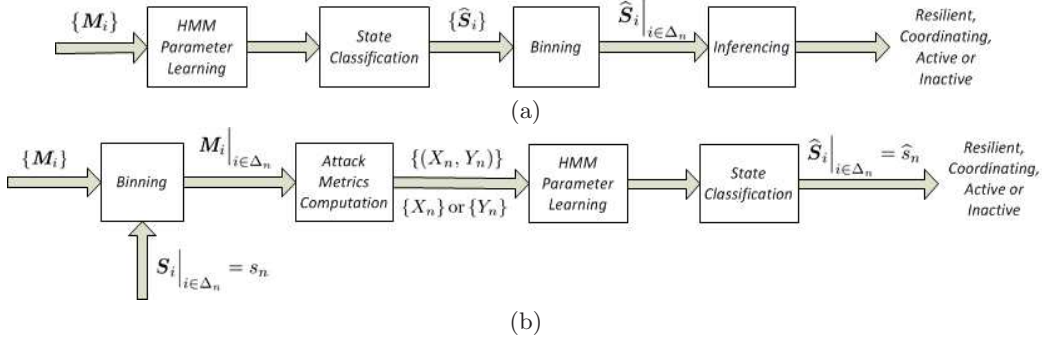


FIG 2. Broad outline of HMM-based parametric approaches: (a) Based on state classification with $\{M_i\}$ as input followed by binning, and (b) Based on binned sets of $\{M_i\}$ as input followed by state classification.

3. Parametric Approaches for Spurt Detection Based on HMM Structure.

The spurt detection problem is similar in objective to the changepoint problem of detecting sudden/abrupt changes in the statistical nature of observations. The theory of changepoint detection has matured significantly and different procedures have been developed (see books by [Basseville and Nikiforov \(1993\)](#); [Tartakovsky, Nikiforov and Basseville \(2014\)](#) for details). Fundamentally speaking, a changepoint procedure is equivalent to an update equation for the test statistic based on the likelihood ratio of the observations. This test statistic is tested against a threshold (which is chosen to meet appropriate false alarm constraints) to lead to a change decision. Developing the structure of the update equation as well as setting the threshold require knowledge of the pre-change and post-change parameters.

A naïve approach to leverage this theory in the context of this work is to ignore the contextual connections between the hidden states and the observations from a terrorist group in developing the update equation for the test statistic of any chosen changepoint procedure, apply it to detect change, and restart it once a change decision (spurt/downfall detection) has been made, so that the next disruption can be monitored. Ignoring the connections between the states and the observations could potentially lead to poor performance in detecting the change as well as poor decisions on changes in group dynamics (such as resilience and coordination) and is thus best avoided.

We now develop approaches that leverage these connections and are tailored to terrorist group dynamics. Toward our goal, we consider the following set of *attack metrics* that capture different attributes of the group: i) X_n , the number of days of terrorist activity, and ii) Y_n , the total number of attacks, both within the Δ_n time-window:

$$(3.1) \quad X_n = \sum_{i \in \Delta_n} \mathbb{1}(M_i > 0); \quad Y_n = \sum_{i \in \Delta_n} M_i, \quad n = 1, 2, \dots, K$$

where $\mathbb{1}(\cdot)$ denotes the indicator function of the set \hat{S}_i under consideration. Note that Y_n/δ is the average number of attacks per day and thus Y_n is a reflection of the intensity of attacks launched by the group. In general, X_n is more indicative of resilience in the group, whereas Y_n captures the level of coordination better.

3.1. *Inferencing with $\{\mathbf{M}_i\}$.* The simplest method to leverage the underlying HMM structure and develop a parametric scheme to classify the hidden states is illustrated in Fig. 2(a) and is described as follows. The observation sequence $\{\mathbf{M}_i\}$, with density as given in (2.1), is used with the classical Baum–Welch algorithm (Rabiner, 1989) to learn the observation density parameters μ_j and γ_j ($j = 0, 1$) as well as the initial probability density (π_0 and π_1) and state transition probability matrix parameters (\mathbf{p}_0 and \mathbf{q}_0); see update equations in Supplementary A. With the converged Baum–Welch parameter estimates as initialization, the Viterbi algorithm (Rabiner, 1989) is then used to estimate the most probable state sequence $\{\widehat{\mathbf{S}}_i\}$ given the observations. At this stage, the states can only be classified as *Active* or *Inactive* ($\widehat{\mathbf{S}}_i \in \{0, 1\}$), with no attribution to any specific mechanism that could result in the corresponding observations. To ensure inferencing on spurts/downfalls and the source of such disruptions (resilience and/or coordination) over disjoint time-windows, one approach is to accumulate the binned state classifications $\widehat{\mathbf{S}}_i \Big|_{i \in \Delta_n}$ and infer on the specific mechanism leading to the observations:

$$(3.2) \quad f\left(\widehat{\mathbf{S}}_i \Big|_{i \in \Delta_n}\right) > \widehat{\eta} \text{ and } g(X_n, Y_n) > \overline{\eta}$$

for an appropriate choice of $f(\cdot)$, $g(\cdot)$, $\widehat{\eta}$ and $\overline{\eta}$ (see Supplementary A for details).

3.2. *Inferencing with $\{(X_n, Y_n)\}$.* In an alternate approach built on $\{X_n\}$ or $\{Y_n\}$ as observation sequence, pictorially illustrated in Fig. 2(b), we assume that the hidden state remains fixed over Δ_n : $\mathbf{S}_i \Big|_{i \in \Delta_n} = s_n$, $s_n \in \{0, 1\}$. The reason for this binning assumption (on the state) is to provide an explicit attribution to macroscopic dynamics in the group unlike the case in Sec. 3.1. Further, the density function of X_n or Y_n becomes difficult to write in closed-form without this assumption. Our goal is to infer s_n with the aid of the appropriate attack metrics corresponding to Δ_n .

Since X_n captures resilience, inferencing² on resilience in the group is performed with $\{X_n\}$ as the observation sequence. Similarly, inferencing on coordination is performed with $\{Y_n\}$, whereas a joint inferencing on the group’s activity is performed with the joint sequence $\{(X_n, Y_n)\}$. With the hurdle-based geometric model in (2.1), the joint density of (X_n, Y_n) is given as (see (Raghavan, Galstyan and Tartakovsky, 2013, Supplementary A) for details)

$$(3.3) \quad \mathbb{P}\left(X_n = k, Y_n = r \mid \mathbf{S}_i \Big|_{i \in \Delta_n} = j\right) = \binom{\delta}{k} \binom{r-1}{r-k} \cdot (1 - \gamma_j)^{\delta-k} (\gamma_j)^k \cdot (1 - \mu_j)^k (\mu_j)^{r-k}, \quad r \geq k.$$

An important property of the density function in (3.3) is that it decomposes into a product of two terms, each depending on only one of the two parameters, γ_j and μ_j . This product structure leads to a simplified update equation for parameter estimation (see Supplementary

²Note that only inferencing with $\{(X_n, Y_n)\}$ is performed in the hurdle-based geometric setting by Raghavan, Galstyan and Tartakovsky (2013). Inferencing with $\{X_n\}$ or $\{Y_n\}$ is not performed due to technical difficulties in deriving update equations. We overcome this difficulty in Supplementary A.

A for details). On the other hand, since X_n counts the number of days of activity, it is a binomial random variable with parameters δ and γ_j :

$$(3.4) \quad \mathbb{P}\left(X_n = k \mid \mathcal{S}_i|_{i \in \Delta_n} = j\right) = \binom{\delta}{k} \cdot (\gamma_j)^k \cdot (1 - \gamma_j)^{\delta - k}.$$

It is to be observed that the above density function depends only on γ_j and hence, inferring of μ_j is impossible with $\{X_n\}$ as the observation sequence. This difficulty is overcome in Supplementary A by using an estimate of μ_j based on all the observations $\{\mathbf{M}_i\}$. Finally, the density function of Y_n is obtained from (3.3) by summing over the k variable:

$$(3.5) \quad \mathbb{P}\left(Y_n = r \mid \mathcal{S}_i|_{i \in \Delta_n} = j\right) = (1 - \gamma_j)^\delta \cdot (\mu_j)^r \cdot \sum_{k=1}^{\min(r, \delta)} \binom{\delta}{k} \binom{r-1}{r-k} \cdot \mathbf{A}^k$$

where $\mathbf{A} = \frac{(1-\mu_j)\gamma_j}{(1-\gamma_j)\mu_j}$. While the above expression can be rewritten in terms of Gauss hypergeometric functions, it appears to be not easily amenable to a closed-form expression rendering a product decomposition (for parameter estimation) in the two parameters difficult, if not impossible; see Supplementary A for details. Under the assumption that $\mu_j > \gamma_j$ (or equivalently, $\mathbf{A} < 1$), update equations for the observation density parameter estimates are obtained in Supplementary A in the $\delta \gg 1$ regime.

State classification is performed using the model parameter estimates from the use of Baum–Welch algorithm on the appropriate observation sequence ($\{X_n\}$, $\{Y_n\}$, or $\{(X_n, Y_n)\}$). The output of the Viterbi algorithm is a state estimate for the period of interest

$$\left\{ \widehat{\mathcal{S}}_i \Big|_{i \in \Delta_n} = \widehat{s}_n \in \{0, 1\} \text{ for all } n = 1, \dots, K \right\}.$$

A state estimate of 1 with $\{X_n\}$ as the observation sequence (correspondingly with $\{Y_n\}$ and the joint sequence $\{(X_n, Y_n)\}$) indicates that the group is resilient (coordinating and both, respectively) over the period of interest, whereas an estimate of 0 indicates that the group is non-resilient (non-coordinating or neither, respectively). Transition between states indicates spurt/downfall in the activity corresponding to the appropriate attribute.

3.3. Difficulties with Parametric Approaches. While both approaches in Sec. 3.1 and Sec. 3.2 exploit the HMM structure in different ways, they also require a reasonable knowledge of the underlying parameter estimates for state classification. Acquiring such knowledge leads to a latency in inferencing. Specific to the context of this work, terrorism incidents are “rare” from the perspective of model learning, even for some of the most active³ terrorist groups. For example, the FARC dataset considered by Raghavan, Galstyan and Tartakovsky (2013) (also in this work) corresponds to 641 incidents over a ten-year period leading to an average of approx. 1.23 incidents per week. Similar trends can be seen across a number of

³While a case can be made that these datasets report only a representative subset of the true activity, the fact that significant amount of resources have to be invested by the terrorist group for every new incident acts as a natural dampener toward more attacks.

terrorist groups, see (LaFree and Dugan, 2007; Breiger et al., 2011; Melamed et al., 2012; Raghavan, 2016) for examples. As a crude illustration, learning a 4 parameter model with 100 observation points (on average) per parameter leads to a model learning latency of $\frac{4 \times 100}{1.23} \approx 325$ weeks or $\approx 6\frac{1}{4}$ years.

A closely related and more challenging problem is the fact that most models capture some underlying attribute of the group dynamics, which in itself can change dramatically over a long time-period (such as that incurred in model learning). This fact renders assumptions of model stability over such periods questionable. The use of the proposed approaches over a long time-horizon (with time-varying parameter estimates) opens up an array of issues on the stability of inferencing decisions in the short time-horizon. The two approaches in Sec. 3.1 and Sec. 3.2 differ as follows. Inferencing with $\{\mathbf{M}_i\}$ is primarily determined by hard decisions ($\{\widehat{\mathbf{S}}_i\}$) that could potentially lead to information loss, unlike inferencing with soft metrics such as $\{(X_n, Y_n)\}$. Nevertheless, both approaches suffer from a common problem which make it unattractive as an *online* approach: a *retrospective (non-causal)* state classification process after model learning.

4. Non-Parametric Approach for Spurt Detection. The above difficulties motivate the development of causal (non-parametric) approaches which is the focus of this section. Non-parametric changepoint procedures based on signs or signed rank statistics of observations with median or Wilcoxon scores have been studied for a long time (see the book by Gibbons and Chakraborti (2011) for a survey). While the utility of such procedures in a terrorist network setting has not been addressed before, we follow along different lines in this work to develop a non-parametric approach that exploits the HMM structure and still competes well with its parametric counterparts in detecting spurts and downfalls. In addition to spurt detection, the proposed approach also identifies the source of disruption behind a spurt/downfall in the activity of a terrorist group. In this approach, instead of using only the summary statistics (X_n and Y_n) of the vector $\mathbf{M}_i \Big|_{i \in \Delta_n}$ as in Sec. 3.2, we consider the entire vector to study resilience and coordination signatures in the group. To develop this approach, recall that resilience and coordination are captured by the group’s ability to perpetrate multiple attacks over successive days and the same day, respectively. Thus, a metric that measures the degree of “well-spreadness” of attacks over Δ_n (or its lack thereof) can be used as an indicator and measure of high resilience (or coordination).

4.1. *Majorization Theory.* With this backdrop, majorization theory provides a theoretical framework (Marshall and Olkin, 1979) to compare two vectors on the basis of their “well-spreadness.” For the sake of self-containment of this paper, a brief introduction to majorization theory, Schur-convex and -concave functions, catalytic majorization, and equivalent conditions for verifying a catalytic majorization relationship between two vectors are provided in Supplementary B. The main conclusion from Supplementary B is provided next.

Let \mathbb{P}_δ denote the space of probability vectors of length δ (where $\delta > 1$) with $\underline{\mathbf{P}} = [\mathbf{P}(1), \dots, \mathbf{P}(\delta)] \in \mathbb{P}_\delta$ if and only if $\mathbf{P}(i) \geq 0$ for all $i = 1, \dots, \delta$ and $\sum_{i=1}^{\delta} \mathbf{P}(i) = 1$. Without loss in generality, we can assume that the entries of $\underline{\mathbf{P}}$ are arranged in non-increasing order (that is, $\mathbf{P}(1) \geq \dots \geq \mathbf{P}(\delta)$).

THEOREM 1. *Let $\{\underline{P}, \underline{Q}\} \in \mathbb{P}_\delta$. In one of two possibilities, \underline{P} and \underline{Q} are not comparable with each other in the form of a catalytic majorization relationship. In the other possibility, their comparability is verified by checking an equivalent set of conditions over only two types of functions:*

- i) $\text{PM}(\underline{P}, \alpha) < \text{PM}(\underline{Q}, \alpha)$ if $\alpha > 1$,
- ii) $\text{PM}(\underline{P}, \alpha) > \text{PM}(\underline{Q}, \alpha)$ if $\alpha < 1$, and
- iii) $\text{SE}(\underline{P}) > \text{SE}(\underline{Q})$.

In the above equations, $\text{SE}(\cdot)$ and $\text{PM}(\cdot, \alpha)$ stand for the Shannon entropy function and the power mean function corresponding to an index α , and are defined as,

$$\text{SE}(\underline{P}) \triangleq - \sum_{i=1}^{\delta} P(i) \log(P(i)), \quad \text{PM}(\underline{P}, \alpha) \triangleq \left(\frac{\sum_{i=1}^{\delta} P(i)^\alpha}{\sum_{i=1}^{\delta} \mathbb{1}(P(i) > 0)} \right)^{1/\alpha}.$$

□

4.2. Computational Reduction by a Single Function Search. While Theorem 1 establishes the importance of evaluating the power mean function over the continuous parameter α in comparing two different vectors, for computational reasons, we propose the search over a single function as proxy. This single function is the normalized power mean corresponding to a fixed index $\alpha^* \geq 1$ (see the definition in Supplementary B as well as a motivation for this functional form as a candidate), which is given as,

$$\text{NPM}(\underline{P}, \alpha^*) = \frac{\text{PM}(\underline{P}, \alpha^*)}{\sum_{i=1}^{\delta} \mathbb{1}(P(i) > 0)} = \frac{\left(\sum_{i=1}^{\delta} P(i)^{\alpha^*} \right)^{1/\alpha^*}}{\left(\sum_{i=1}^{\delta} \mathbb{1}(P(i) > 0) \right)^{1+1/\alpha^*}}.$$

To explain the reason for this specific choice, we define $\alpha_{\max}(\text{PM})$ and $\alpha_{\max}(\text{NPM})$ corresponding to \underline{P} and \underline{Q} (suitably permuted) as follows:

$$\begin{aligned} \alpha_{\max}(\text{PM}) &\triangleq \arg \sup_{\alpha \in [1, \infty)} \left\{ \text{PM}(\underline{P}, \alpha) > \text{PM}(\underline{Q}, \alpha) \right. \\ &\quad \left. \text{and } \text{PM}(\underline{P}, \tilde{\alpha}) \leq \text{PM}(\underline{Q}, \tilde{\alpha}) \text{ for all } \tilde{\alpha} > \alpha \right\} \\ \alpha_{\max}(\text{NPM}) &\triangleq \arg \sup_{\alpha \in [1, \infty)} \left\{ \text{NPM}(\underline{P}, \alpha) > \text{NPM}(\underline{Q}, \alpha) \right. \\ &\quad \left. \text{and } \text{NPM}(\underline{P}, \tilde{\alpha}) \leq \text{NPM}(\underline{Q}, \tilde{\alpha}) \text{ for all } \tilde{\alpha} > \alpha \right\}. \end{aligned}$$

In other words, $\alpha_{\max}(\cdot)$ is the largest choice (supremum) of α at which the inequality relationship desired in Theorem 1 fails to hold (for the corresponding function) with \underline{P} and

\underline{Q} as inputs. Similarly, we define $\alpha_{\min}(\text{PM})$ and $\alpha_{\min}(\text{NPM})$, corresponding to the smallest choice (infimum) of α at which the inequality relationship of Theorem 1 fails to hold, as:

$$\begin{aligned} \alpha_{\min}(\text{PM}) &\triangleq \arg \inf_{\alpha \in (-\infty, 1]} \left\{ \text{PM}(\underline{P}, \alpha) < \text{PM}(\underline{Q}, \alpha) \right. \\ &\quad \left. \text{and } \text{PM}(\underline{P}, \tilde{\alpha}) \geq \text{PM}(\underline{Q}, \tilde{\alpha}) \text{ for all } \tilde{\alpha} < \alpha \right\} \\ \alpha_{\min}(\text{NPM}) &\triangleq \arg \inf_{\alpha \in (-\infty, 1]} \left\{ \text{NPM}(\underline{P}, \alpha) < \text{NPM}(\underline{Q}, \alpha) \right. \\ &\quad \left. \text{and } \text{NPM}(\underline{P}, \tilde{\alpha}) \geq \text{NPM}(\underline{Q}, \tilde{\alpha}) \text{ for all } \tilde{\alpha} < \alpha \right\}. \end{aligned}$$

Note that $\alpha_{\max}(\text{PM})$ is well-defined since

$$\lim_{\alpha \rightarrow \infty} \text{PM}(\underline{P}, \alpha) - \text{PM}(\underline{Q}, \alpha) = P(1) - Q(1)$$

and this quantity can be ensured to be upper bounded by 0 after an appropriate permutation of \underline{P} and \underline{Q} . Similarly, $\alpha_{\max}(\text{NPM})$ is well-defined since

$$\lim_{\alpha \rightarrow \infty} \text{NPM}(\underline{P}, \alpha) - \text{NPM}(\underline{Q}, \alpha) = \frac{P(1)}{\sum_{i=1}^{\delta} \mathbb{1}(P(i) > 0)} - \frac{Q(1)}{\sum_{i=1}^{\delta} \mathbb{1}(Q(i) > 0)}.$$

As before, the quantity above can also be ensured to be upper bounded by 0 after an appropriate permutation (but not perhaps the same permutation as in the previous case). Similarly, $\alpha_{\min}(\text{PM})$ and $\alpha_{\min}(\text{NPM})$ are also well-defined since we have

$$\begin{aligned} \lim_{\alpha \rightarrow -\infty} \text{PM}(\underline{P}, \alpha) - \text{PM}(\underline{Q}, \alpha) &= P(\delta) - Q(\delta) \\ \lim_{\alpha \rightarrow -\infty} \text{NPM}(\underline{P}, \alpha) - \text{NPM}(\underline{Q}, \alpha) &= \frac{P(\delta)}{\sum_{i=1}^{\delta} \mathbb{1}(P(i) > 0)} - \frac{Q(\delta)}{\sum_{i=1}^{\delta} \mathbb{1}(Q(i) > 0)}, \end{aligned}$$

both of which can be lower bounded by 0 with appropriate permutations of \underline{P} and \underline{Q} .

Specifically, if $\underline{P} \prec \underline{Q}$, (from Prop. 1 and Corollary 1 of Supplementary B) we have $\{\alpha_{\max}(\text{PM}), \alpha_{\max}(\text{NPM}), \alpha_{\min}(\text{PM})\} = 1$. In general, if $\underline{P} \not\prec \underline{Q}$, we can have the following possibilities: $\{\alpha_{\max}(\text{PM}), \alpha_{\max}(\text{NPM})\} > 1$ and $\{\alpha_{\min}(\text{PM}), \alpha_{\min}(\text{NPM})\} < 1$. To understand the precise behavior of these quantities and the relative frequency of the event where $\{\alpha_{\max}(\text{PM}), \alpha_{\max}(\text{NPM})\} > 1$ and $\{\alpha_{\min}(\text{PM}), \alpha_{\min}(\text{NPM})\} < 1$, we now study the cumulative distribution function (CDF) of $\alpha_{\max}(\cdot)$ and $\alpha_{\min}(\cdot)$ with three random models for generating \underline{P} and \underline{Q} . In all the models, we have $\underline{P} \in \mathbb{P}_{\delta_1}$ and $\underline{Q} \in \mathbb{P}_{\delta_2}$ where δ_1 and δ_2 are (discrete) uniformly distributed as $\{\delta_1, \delta_2\} \sim \mathcal{U}([1, \delta])$. The non-zero entries of \underline{P} and \underline{Q} (which are yet to be permuted in non-increasing order) are generated as

$$P(i) = \frac{p_i}{\sum_{j=1}^{\delta_1} p_j}, \quad i = 1, \dots, \delta_1, \quad Q(i) = \frac{q_i}{\sum_{j=1}^{\delta_2} q_j}, \quad i = 1, \dots, \delta_2$$

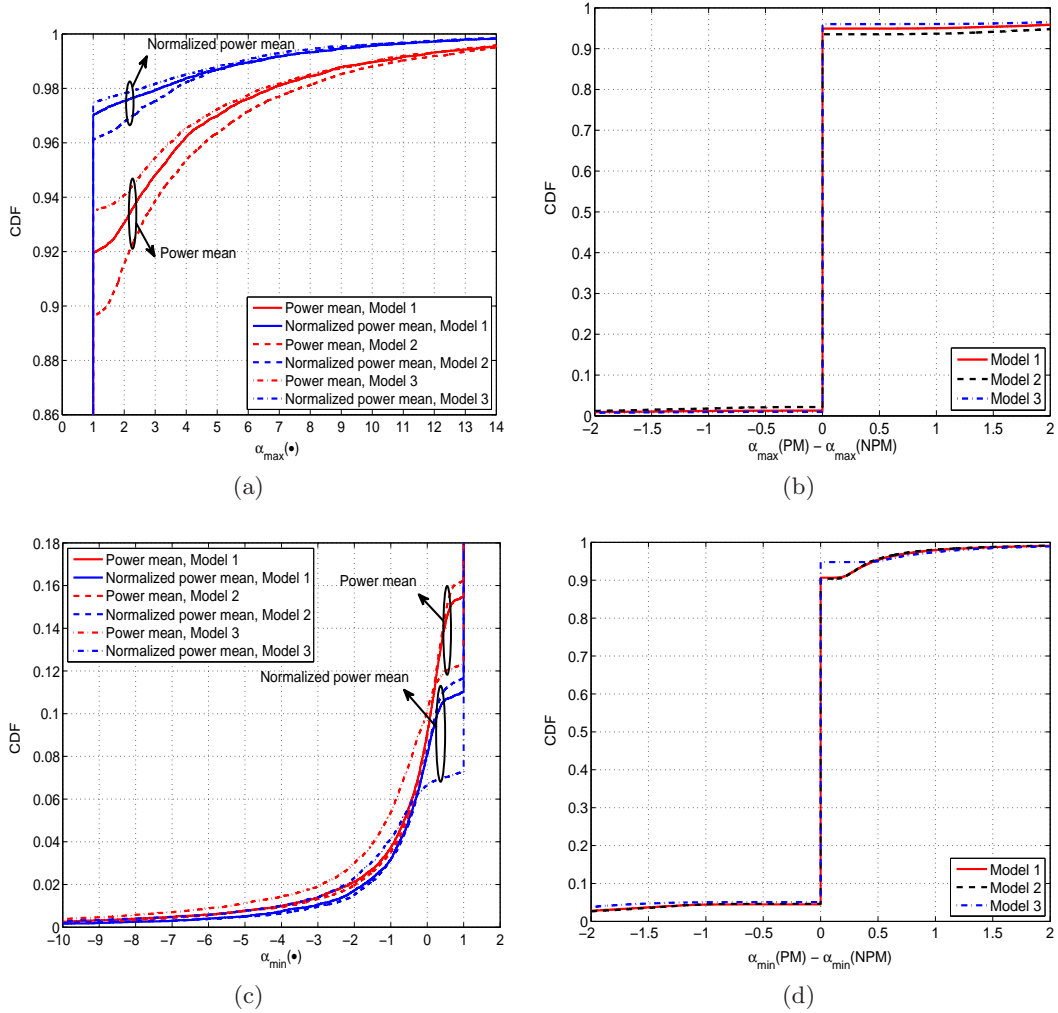


FIG 3. CDF of: (a) $\alpha_{\max}(\text{PM})$ and $\alpha_{\max}(\text{NPM})$, (b) $\alpha_{\max}(\text{PM}) - \alpha_{\max}(\text{NPM})$, (c) $\alpha_{\min}(\text{PM})$ and $\alpha_{\min}(\text{NPM})$, and (d) $\alpha_{\min}(\text{PM}) - \alpha_{\min}(\text{NPM})$ with $\delta = 7$ and $K = 10$ for three random models generating \underline{P} and \underline{Q} .

where $\{p_i, q_i\}$ are from one of the three models below (continuous uniform, folded normal and discrete uniform):

$$\begin{aligned} \text{Model 1} &: \{p_i, q_i\} \sim \mathcal{U}([0, 1]) \\ \text{Model 2} &: \{p_i, q_i\} \sim |\mathcal{N}| \\ \text{Model 3} &: \{p_i, q_i\} \sim \mathcal{U}([1, K]). \end{aligned}$$

Fig. 3(a) plots the CDF of $\alpha_{\max}(\text{PM})$ and $\alpha_{\max}(\text{NPM})$ for the three models with $\delta = 7$ days and $K = 10$. Clearly, $\alpha_{\max}(\text{PM})$ and $\alpha_{\max}(\text{NPM})$ are 1 for a large fraction (over 90%)

of the realizations of $\{\underline{P}, \underline{Q}\}$ suggesting⁴ that these realizations can be compared in a catalytic majorization relationship. We also observe that, for a fixed α , the normalized power mean can be used to discern \underline{P} and \underline{Q} better in the sense that this metric allows a comparative relationship for a larger fraction of the realizations than the power mean. Fig. 3(b) plots the CDF of $\alpha_{\max}(\text{PM}) - \alpha_{\max}(\text{NPM})$ for the three models which also shows that while $\alpha_{\max}(\text{PM}) = 1 = \alpha_{\max}(\text{NPM})$ in a large fraction (over 95%) of the cases, the normalized power mean is more effective than the power mean reflected by the higher probability for the event where $\alpha_{\max}(\text{PM})$ is larger than $\alpha_{\max}(\text{NPM})$ than for the event where $\alpha_{\max}(\text{PM})$ is smaller than $\alpha_{\max}(\text{NPM})$. Similar trends can be seen in Figs. 3(c)-(d) for $\{\alpha_{\min}(\text{PM}), \alpha_{\min}(\text{NPM})\}$ and $\alpha_{\min}(\text{PM}) - \alpha_{\min}(\text{NPM})$.

While Fig. 3 does not conclusively establish the efficacy of the normalized power mean (relative to the power mean) for a single function search as proxy, a further study illustrated in Table 1 provides this evidence. In this table, we list the conditional probability $P_{\text{PM}}(\alpha^*)$ (the definition for $P_{\text{NPM}}(\alpha^*)$ follows analogously) that all the inequality relationships in Theorem 1 are satisfied provided the corresponding inequality relationship with the proxy function is satisfied:

$$P_{\text{PM}}(\alpha^*) = \begin{cases} P\left(\text{PM}(\underline{P}, \alpha) \leq \text{PM}(\underline{Q}, \alpha) \text{ for all } \alpha \geq 1 \text{ and } \text{PM}(\underline{P}, \alpha) \geq \text{PM}(\underline{Q}, \alpha) \right. \\ \quad \left. \text{for all } \alpha \leq 1 \mid \text{PM}(\underline{P}, \alpha^*) \leq \text{PM}(\underline{Q}, \alpha^*) \right) \text{ if } \alpha^* \geq 1 \\ P\left(\text{PM}(\underline{P}, \alpha) \leq \text{PM}(\underline{Q}, \alpha) \text{ for all } \alpha \geq 1 \text{ and } \text{PM}(\underline{P}, \alpha) \geq \text{PM}(\underline{Q}, \alpha) \right. \\ \quad \left. \text{for all } \alpha \leq 1 \mid \text{PM}(\underline{P}, \alpha^*) \geq \text{PM}(\underline{Q}, \alpha^*) \right) \text{ if } \alpha^* \leq 1. \end{cases}$$

Recall that the standard error for a probability estimate \hat{p} with n samples used to estimate this probability is given as $\sqrt{\frac{\hat{p}(1-\hat{p})}{n}}$. While Table 1 corresponds to $\delta = 7$, $K = 10$ and $K = 15$, similar patterns are seen with $\delta = 10$ and $\delta = 14$ as well (data not provided here for space reasons). From Table 1, we note that the efficacy of a single function search with a larger α^* is in general better than a check with a smaller α^* . Further, the normalized power mean discerns the comparability between two vectors more effectively than the power mean with $\alpha^* = 1$ and $\alpha^* = 2$ allowing the comparison of over 90% of the realizations of $\{\underline{P}, \underline{Q}\}$ suggesting their utility here. We use the choice $\alpha^* = 2$ in the rest of the sequel for illustrative purposes.

4.3. Appropriate Function for Resilience and Coordination Monitoring. With Shannon entropy and normalized power mean corresponding to a fixed index α^* as candidate functions, we now illustrate the importance of one function (over the other) depending on whether the goal is to measure changes in resilience or coordination.

In the first case study, we consider the scenario where K attacks are spread over Δ_n in different ways: $K - k$ attacks on one day and k days with one attack on each day (where

⁴This is not conclusively established since Conditions ii) and iii) of Theorem 1 have not been verified.

TABLE 1

Conditional probability with their standard errors in parentheses capturing efficacy of a single function search. Largest conditional probability values are highlighted in bold-face.

α^*	$P_{PM}(\alpha^*)$				$P_{NPM}(\alpha^*)$			
	-1	0	1	2	-1	0	1	2
Model 1	0.7016 (0.0030)	0.7412 (0.0029)	0.8797 (0.0024)	0.8895 (0.0023)	0.7939 (0.0026)	0.8364 (0.0025)	0.9498 (0.0015)	0.9527 (0.0015)
Model 2	0.6689 (0.0031)	0.7075 (0.0030)	0.8461 (0.0026)	0.8606 (0.0026)	0.7753 (0.0027)	0.8205 (0.0026)	0.9359 (0.0017)	0.9360 (0.0017)
Model 3, $K = 10$	0.7598 (0.0028)	0.7994 (0.0027)	0.9139 (0.0020)	0.9002 (0.0021)	0.8465 (0.0024)	0.8678 (0.0022)	0.9720 (0.0012)	0.9563 (0.0014)
Model 3, $K = 15$	0.7386 (0.0029)	0.7807 (0.0028)	0.9072 (0.0021)	0.8939 (0.0022)	0.8318 (0.0024)	0.8600 (0.0023)	0.9711 (0.0012)	0.9543 (0.0015)

$k \in [0, \delta - 1]$) corresponding to an *attack frequency vector*

$$\underline{P}_k = \frac{1}{K} \cdot \left[K - k, \underbrace{1, \dots, 1}_{k \text{ times}}, \underbrace{0, \dots, 0}_{\delta - (k+1) \text{ times}} \right].$$

The attack frequency vector captures the distribution of frequency of attacks over Δ_n and by definition, $\underline{P}_k \in \mathbb{P}_\delta$ provided that there is at least one attack over Δ_n . With $k = 0$, the group is highly coordinating since all the attacks are clustered on one day. With $k = \delta - 1$, the group is resilient since the attacks are well-spread over Δ_n . In general, as k increases, the coordination in the group decreases and its resilience increases.

We consider two benchmark attack frequency vectors \underline{P}_c and \underline{P}_r to compare the efficacy of the two majorization metrics (Shannon entropy and normalized power mean corresponding to an index α^*) in measuring changes in the group dynamics with \underline{P}_k :

$$\underline{P}_c = \left[1, \underbrace{0, \dots, 0}_{\delta - 1 \text{ times}} \right], \quad \underline{P}_r = \left[\underbrace{1/\delta, \dots, 1/\delta}_{\delta \text{ times}} \right].$$

The majorization metrics considered for comparison are the differences in Shannon entropy and normalized power mean with \underline{P}_k and the benchmark vectors:

$$\begin{aligned} \Delta SE_r(k) &\triangleq \left| SE(\underline{P}_r) - SE(\underline{P}_k) \right| \\ \Delta SE_c(k) &\triangleq \left| SE(\underline{P}_c) - SE(\underline{P}_k) \right| \\ \Delta NPM_r(k) &\triangleq \left| NPM(\underline{P}_r, \alpha^*) - NPM(\underline{P}_k, \alpha^*) \right| \\ \Delta NPM_c(k) &\triangleq \left| NPM(\underline{P}_c, \alpha^*) - NPM(\underline{P}_k, \alpha^*) \right|. \end{aligned}$$

In Fig. 4(a), $\Delta SE_r(k)$ and $\Delta NPM_r(k)$ are plotted with $\delta = 7$, $\alpha^* = 2$, and $K = 10, 15$ and 20. From this study, we observe that the Shannon entropy captures a change in a resilient group (large k regime) better with a higher ΔSE value than ΔNPM . Similarly, in Fig. 4(b),

$\Delta\text{SE}_c(k)$ and $\Delta\text{NPM}_c(k)$ are plotted and the normalized power mean captures a change in a coordinating group (small k regime) better with a higher ΔNPM value than ΔSE .

We then consider a second case study where k attacks are equally spread over k days in the Δ_n time-period corresponding to an attack frequency vector

$$\underline{\mathbf{P}}_k = \left[\underbrace{\frac{1}{k}, \dots, \frac{1}{k}}_{k \text{ times}}, \underbrace{0, \dots, 0}_{\delta-k \text{ times}} \right].$$

Clearly, $\text{SE}(\underline{\mathbf{P}}_k) = \log(k)$ and $\text{NPM}(\underline{\mathbf{P}}_k, \alpha^*) = \frac{1}{k^2}$ for any α^* . Further, it can be seen that

$$\begin{aligned} \left| \frac{\partial}{\partial k} \text{SE}(\underline{\mathbf{P}}_k) \right| &= \frac{1}{k} < \frac{2}{k^3} = \left| \frac{\partial}{\partial k} \text{NPM}(\underline{\mathbf{P}}_k, \alpha^*) \right| && \text{for small } k \\ \left| \frac{\partial}{\partial k} \text{SE}(\underline{\mathbf{P}}_k) \right| &= \frac{1}{k} > \frac{2}{k^3} = \left| \frac{\partial}{\partial k} \text{NPM}(\underline{\mathbf{P}}_k, \alpha^*) \right| && \text{for large } k, \end{aligned}$$

suggesting the relevance of Shannon entropy for capturing changes in resilience (large k regime) and normalized power mean for capturing changes in coordination (small k regime).

4.4. *Application to Spurt/Downfall Detection.* We now apply the framework developed in Sec. 4.1 to Sec. 4.3 to track changes in resilience and coordination in the group. For this, let $\underline{\mathbf{P}}_n = [\mathbf{P}_n(1), \dots, \mathbf{P}_n(\delta)]$ where

$$\mathbf{P}_n(i) = \begin{cases} \frac{M_{(n-1)\delta+i}}{\sum_{j \in \Delta_n} M_j} & \text{if } \sum_{j \in \Delta_n} M_j > 0, \\ 0 & \text{otherwise} \end{cases}$$

denote the attack frequency vector over the time-window Δ_n . In the non-trivial setting of at least one attack over Δ_n , the Shannon entropy and normalized power mean reduce to

$$\begin{aligned} \text{SE}(\underline{\mathbf{P}}_n) &= \log \left(\sum_{i \in \Delta_n} M_i \right) - \frac{\sum_{i \in \Delta_n} M_i \log(M_i)}{\sum_{i \in \Delta_n} M_i} \\ \text{NPM}(\underline{\mathbf{P}}_n, \alpha^*) &= \frac{\left(\sum_{i \in \Delta_n} (M_i)^{\alpha^*} \right)^{1/\alpha^*}}{\left(\sum_{i \in \Delta_n} M_i \right) \cdot \left(\sum_{i \in \Delta_n} \mathbb{1}(M_i > 0) \right)^{1+1/\alpha^*}}, \end{aligned}$$

respectively. In the trivial setting of no attacks over Δ_n , we set $\underline{\mathbf{P}}_n = [0, \dots, 0]$ and $\text{SE}(\underline{\mathbf{P}}_n) = 0 = \text{NPM}(\underline{\mathbf{P}}_n, \alpha^*)$. With these metrics, resilience and coordination in the group over the n th time-window are declared based on the satisfaction of the following conditions:

$$(4.1) \quad \text{Resilient} \iff \text{SE}(\underline{\mathbf{P}}_n) > \underline{\text{SE}} \text{ and } X_n > \tilde{\eta}_X$$

$$(4.2) \quad \text{Coordinating} \iff \text{NPM}(\underline{\mathbf{P}}_n, \alpha^*) > \underline{\text{NPM}} \text{ and } Y_n > \tilde{\eta}_Y$$

corresponding to appropriate choices of $\tilde{\eta}_X$, $\tilde{\eta}_Y$, $\underline{\text{SE}}$ and $\underline{\text{NPM}}$.

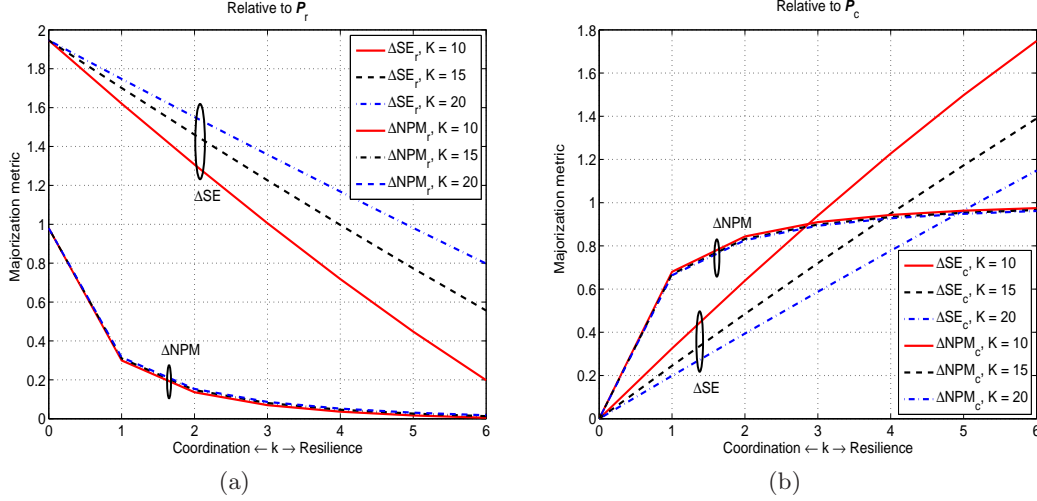


FIG 4. Majorization metrics plotted relative to (a) \underline{P}_r and (b) \underline{P}_c as the attack frequency vector \underline{P}_k transitions from more coordinating to more resilient.

In addition to classification, we are interested in tracking the resilience and coordination in the group over time. For this, we propose two tracking functions ($\text{Res}(n)$ and $\text{Coord}(n)$, $n \geq 1$) that are updated as follows:

$$\text{Res}(n) = \text{Res}(n-1) + \text{SE}(\underline{P}_n) + X_n - \frac{\sum_{n'=1}^{N_{\max}} (\text{SE}(\underline{P}_{n'}) + X_{n'})}{N_{\max}}$$

$$\text{Coord}(n) = \text{Coord}(n-1) + \text{NPM}(\underline{P}_n, \alpha^*) + Y_n - \frac{\sum_{n'=1}^{N_{\max}} (\text{NPM}(\underline{P}_{n'}, \alpha^*) + Y_{n'})}{N_{\max}}$$

with $\text{Res}(0) = 0 = \text{Coord}(0)$. It can be checked that $\text{Res}(N_{\max}) = 0 = \text{Coord}(N_{\max})$ and thus these choices of tracking functions allow comparison of resilience and coordination in the group relative to long-term trends (captured by the time-index N_{\max}) by choosing N_{\max} sufficiently large and appropriately.

5. Numerical Studies. We now illustrate the efficacy of the proposed theoretical framework with various numerical studies. In the first numerical study, activity data from a two-state HMM framework with a hurdle-based geometric model corresponding to $\mathbf{p}_0 = 0.4$, $\mathbf{q}_0 = 0.6$, $\gamma_0 = 0.1$, $\mu_0 = 0.3$, $\gamma_1 = 0.2$ and $\mu_1 = 0.4$ is generated over $N = 1500 \cdot \delta$ days where $\delta = 7$ (or approximately 29 years). The number of days of activity and number of attacks over the first 500 time-windows of this period are plotted in Fig. 5(a). Based on correlations between X_n and resilience (and Y_n and coordination), we declare⁵ that the

⁵The choices of the parameter settings are motivated by a comparative analysis of the trends of many terrorist groups. The scope of this discussion is left for a separate work; see (Raghavan, 2016).

group is resilient or coordinating provided the following conditions are satisfied:

$$\text{Resilient} \iff X_n > \eta_X = 3 \text{ and } \mathbf{S}_i \Big|_{i \in \Delta_n} = 1$$

$$\text{Coordinating} \iff Y_n > \eta_Y = 6 \text{ and } \mathbf{S}_i \Big|_{i \in \Delta_n} = 1$$

$$\text{Both resilient and coordinating} \iff X_n > \eta_X = 3, Y_n > \eta_Y = 6 \text{ and } \mathbf{S}_i \Big|_{i \in \Delta_n} = 1.$$

The above classification leads to 24, 26 and 10 time-windows over which the activity data is resilient, coordinating, and both resilient and coordinating, respectively. This classification serves as “the ground truth” against which we compare the performance of different algorithms subsequently. The nature of the states (resilient, coordinating, or both, *Active* or *Inactive*) over the first 500 time-windows are also plotted in Fig. 5(a).

With $\{\mathbf{M}_i\}$ as observations, model parameters are learned with the Baum-Welch algorithm (see parameter estimates in Table 2) and with these estimates, states (over each day) are classified as *Active* or *Inactive* using the Viterbi algorithm. Time-windows are then classified as resilient or coordinating with the following classification parameter settings⁶ in Supplementary A: $\hat{\eta}_X = 3$, $\hat{\eta}_Y = 5$ and $\hat{\eta} = 3$. Similarly, $\{X_n\}$, $\{Y_n\}$ and $\{(X_n, Y_n)\}$ are used as observations for parameter learning (see parameter estimates in Table 2) and the resultant parameter estimates are fed into the Viterbi algorithm for classifying time-windows as resilient, coordinating, or both resilient and coordinating, respectively. On the other hand, the majorization theory-based approach classifies time-windows as resilient and/or coordinating with parameter settings in (4.1)-(4.2) for classification chosen as $\tilde{\eta}_X = 3$, $\tilde{\eta}_Y = 6$, $\underline{\text{SE}} = 1$ and $\underline{\text{NPM}} = 0.0625$.

To provide metrics on the performance of the different state classification algorithms, we define a *missed detection* event as a time-window in the resilient/coordinating state (as per “the ground truth”) that is not declared to be so by the state classification algorithm. Similarly, a *false alarm* event corresponds to a time-window that is declared as resilient/coordinating when it is not one (as per “the ground truth”). The probability of missed detection (P_{MD}) and probability of false alarm (P_{FA}) are defined as the fraction of true events not declared to be so by the classification algorithm and fraction of classified events that are not true events, respectively.

Table 2 provides a summary statistics of missed detection and false alarm events with the different state classification algorithms as well as the parameter estimates. From Table 2, we note that the learned model parameters are similar with different sets of observations. Learning with $\{\mathbf{M}_i\}$ results in good resilience decisions with no miss of true events and a low false alarm probability. However, $\{\mathbf{M}_i\}$ leads to poor coordination decisions with a number of misses and false alarms. On the other hand, learning with $\{X_n\}$ or $\{Y_n\}$ or $\{(X_n, Y_n)\}$ results in no misses of a true resilience/coordination event, but these approaches lead to a considerably large number of false alarms. Further, all these decisions come at the cost

⁶Optimizing the choice of the classification parameter settings is a task of importance that is left for a follow-up work. The main purpose of this work is to illustrate the utility of the proposed ideas rather than to fine-tune the algorithms extensively over the parameter space.

of model learning latencies. On the other hand, the majorization theory-based approach leads to a low miss and false alarm probability by tuning to the appropriate signature for monitoring. The corresponding state classifications with these approaches for resilience and coordination over the first 500 time-windows are presented in Figs. 5(b)-(c), respectively.

In addition, Fig. 5(d) plots the resilience and coordination tracking functions of the group over the first 500 time-windows with $N_{\max} = 1500$. From this plot, while resilience and coordination follow similar macroscopic patterns, we can also obtain general indicators as to whether resilience increases first (or coordination increases first). Notable indicators of the group's behavior include: resilience in the group increases first while coordination remains stable (around 20-30 time-windows), coordination increases while resilience diminishes (around 60-70 time-windows), both features diminish (90-130 time-windows) followed by a spurt and further diminishing (140-220 time-windows), an increase in both resilience and coordination (220-250 time-windows) followed by general diminishing (250-300 time-windows) and a general spurt (300-450 time-windows), and a spurt in coordination at around the 450th time-window followed by a spurt in resilience. Thus, the tracking functions provide a close glimpse in terms of the group's *Capabilities* over time. While similar classifications and tracking have been proposed by Bakker, Raab and Milward (2012) and Cragin and Daly (2004), our work differs from these prior works by developing a theoretical (and automated) framework to classify and track resilience and coordination in the group instead of depending on subject-matter experts for classification.

In the next numerical study, real terrorism data from RDWTI on the FARC terrorist group over a time-period of 3640 days (or 520 time-windows with $\delta = 7$ days) over the 1998-2007 period is considered. States are classified as resilient, coordinating, or both resilient and coordinating according to a certain manual classification procedure that correlates with spurts in X_n , Y_n and (X_n, Y_n) , respectively. Model parameters are learned with $\{\mathbf{M}_i\}$, $\{X_n\}$, $\{Y_n\}$ and $\{(X_n, Y_n)\}$ as observations and states are classified with the following classification parameter settings: $\hat{\eta}_X = 3$, $\hat{\eta}_Y = 5$ and $\hat{\eta} = 3$. Similarly, states are classified with the majorization theory-based approach using $\tilde{\eta}_X = 3$, $\tilde{\eta}_Y = 5$, $\underline{SE} = 1$ and $\underline{NPM} = 0.0204$. Analogous to Fig. 5, Figs. 6(a)-(c) plot the resilient and coordinating state classifications, whereas Fig. 6(d) plots the resilience and coordination tracking functions corresponding to $N_{\max} = 520$ for FARC. Table 2 also provides a summary statistics of missed detection and false alarm events with the different state classification algorithms as well as the parameter estimates. Clearly, we see that the majorization theory-based approach performs as well as (or better than) the parametric approach based on $\{\mathbf{M}_i\}$, $\{X_n\}$, $\{Y_n\}$, or $\{(X_n, Y_n)\}$. Further, the tracking functions capture the two major spurts in resilience and coordination in the group, as well as the relative growth/decay in these attributes over time; see (Raghavan, Galstyan and Tartakovsky, 2013, Supplementary B) and (Cragin and Daly, 2004) for an explanation.

6. Concluding Remarks. In the light of recent interest in modeling and monitoring of terrorist activity, this work focussed on detecting sudden spurts in the activity profile of terrorist groups. Most work in this area are parametric in nature, which renders their real-life application difficult. In particular, parametric approaches to spurt detection often rely

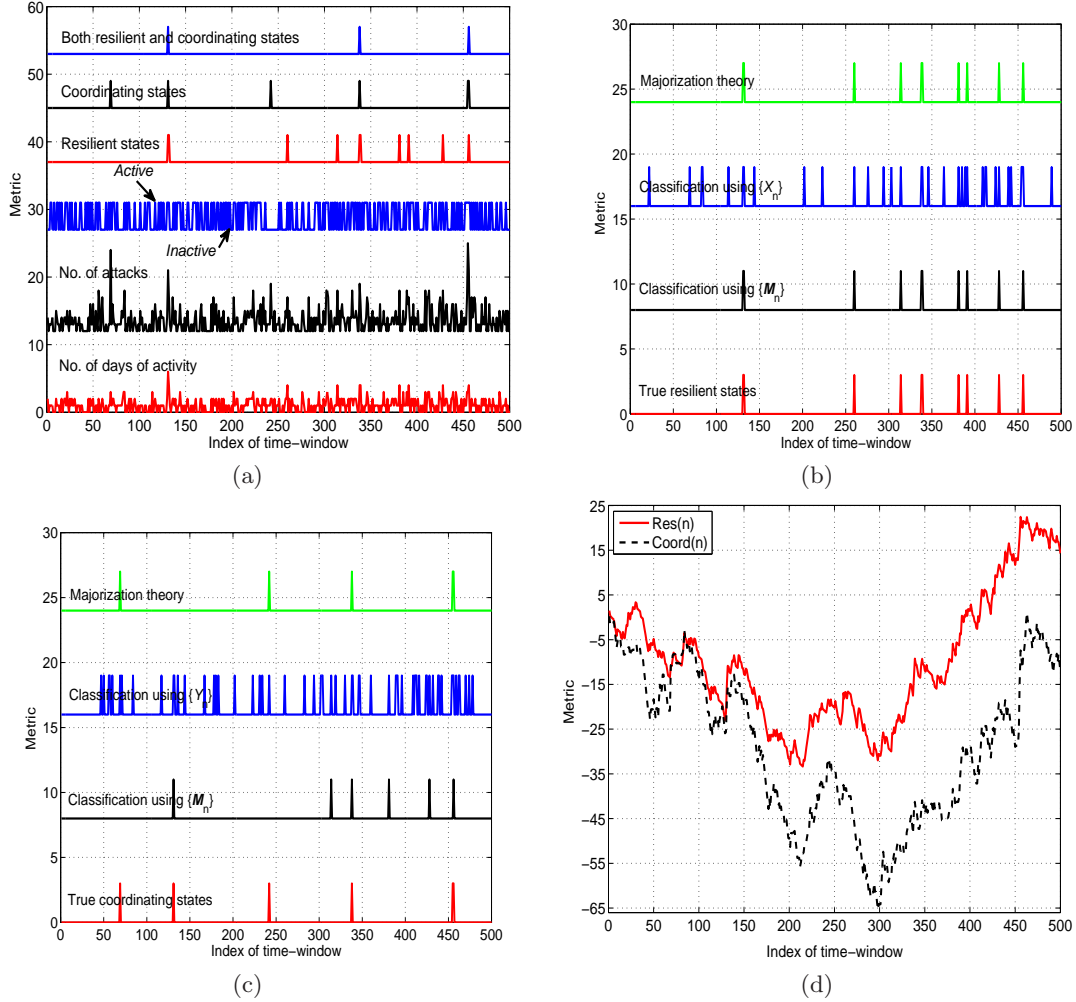


FIG 5. (a) Number of days of activity, number of attacks, true Active, resilient and coordinating states, (b) Resilient and (c) Coordinating state classification with different algorithms, and (d) Resilience and coordination tracking functions over the first 500 time-windows.

on past behavior for prediction, but terrorists' behavior changes quickly enough to make some of this analysis useless. To overcome this fundamental difficulty, we proposed a non-parametric approach based on majorization theory to detect sudden and abrupt changes in the *Capabilities* of the group. Leveraging the notion of catalytic majorization, we developed a simple approach to increment/decrement an appropriate statistic that captures different facets of the terrorist group (such as resilience and level of coordination) in this work. Future work will consider the application of this approach to a broad swathe of terrorist groups' activity profiles as well as applications in social network settings.

TABLE 2

Probabilities of missed detection and false alarm with different state classification algorithms for the data generated from a hurdle-based geometric model and for FARC data.

Data from hurdle-based geometric model				
Setting	Parameters	Number of states classified and (P_{MD}, P_{FA})		
		Resilient	Coordinating	Both
True Observations	$\gamma_0 = 0.1, \mu_0 = 0.3$ $\gamma_1 = 0.2, \mu_1 = 0.4$	24	26	10
Learning with $\{M_i\}$	$\hat{\gamma}_0 = 0.1058, \hat{\mu}_0 = 0.3042$ $\hat{\gamma}_1 = 0.3861, \hat{\mu}_1 = 0.4433$	26 (0, 0.0769)	15 (0.6154, 0.3333)	15 (0, 0.3333)
Learning with $\{X_n\}$	$\hat{\gamma}_0 = 0.1295, \hat{\mu}_0 = 0.4776$ $\hat{\gamma}_1 = 0.2719, \hat{\mu}_1 = 0.4776$	101 (0, 0.7624)	–	–
Learning with $\{Y_n\}$	$\hat{\gamma}_0 = 0.1515, \hat{\mu}_0 = 0.2019$ $\hat{\gamma}_1 = 0.2528, \hat{\mu}_1 = 0.5287$	–	192 (0, 0.8646)	–
Learning with $\{(X_n, Y_n)\}$	$\hat{\gamma}_0 = 0.1306, \hat{\mu}_0 = 0.3286$ $\hat{\gamma}_1 = 0.2553, \hat{\mu}_1 = 0.4797$	–	–	127 (0, 0.9213)
Majorization theory	–	26 (0, 0.0769)	27 (0.0769, 0.1111)	8 (0.2000, 0)
FARC data				
Setting	Parameters	Number of states classified and (P_{MD}, P_{FA})		
		Resilient	Coordinating	Both
True Observations	–	37	18	14
Learning with $\{M_i\}$	$\hat{\gamma}_0 = 0.0953, \hat{\mu}_0 = 0.0762$ $\hat{\gamma}_1 = 0.3988, \hat{\mu}_1 = 0.3087$	27 (0.2703, 0)	13 (0.3889, 0.1538)	13 (0.2143, 0.1538)
Learning with $\{X_n\}$	$\hat{\gamma}_0 = 0.0933, \hat{\mu}_0 = 0.3505$ $\hat{\gamma}_1 = 0.3921, \hat{\mu}_1 = 0.3505$	125 (0, 0.7040)	–	–
Learning with $\{Y_n\}$	$\hat{\gamma}_0 = 0.0951, \hat{\mu}_0 = 0.1232$ $\hat{\gamma}_1 = 0.2500, \hat{\mu}_1 = 0.5745$	–	73 (0, 0.7534)	–
Learning with $\{(X_n, Y_n)\}$	$\hat{\gamma}_0 = 0.0949, \hat{\mu}_0 = 0.0752$ $\hat{\gamma}_1 = 0.3958, \hat{\mu}_1 = 0.3082$	–	–	73 (0, 0.8082)
Majorization theory	–	27 (0.2703, 0)	15 (0.2778, 0.1333)	13 (0.2143, 0.1538)

SUPPLEMENTARY MATERIAL

Supplementary A: Update equations for the Baum-Welch algorithm

(; .pdf). This section derives the update equations for model parameter learning and mechanism association with different types of approaches within the HMM framework.

We now develop update equations for the observation density parameters ($\hat{\gamma}_j$ and $\hat{\mu}_j$) when Baum-Welch algorithm (Rabiner, 1989) is applied to a training-set of N observations $\mathcal{O} = \{O_n, n = 1, \dots, N\}$. Let the corresponding hidden states be given as $\mathcal{S} = \{S_n, n = 1, \dots, N\}$ with S_0 initialized according to an initial probability density $\{\pi_j, j = 0, 1\}$. The Baum auxiliary function with current/initial estimate of HMM parameters $\bar{\lambda}$ as a function of the optimization variable λ , denoted as $Q(\lambda, \bar{\lambda})$, is given as:

$$Q(\lambda, \bar{\lambda}) \triangleq \sum_{\mathcal{S}} \log \left(P(\mathcal{O}, \mathcal{S} | \lambda) \right) \cdot P(\mathcal{O}, \mathcal{S} | \bar{\lambda}).$$

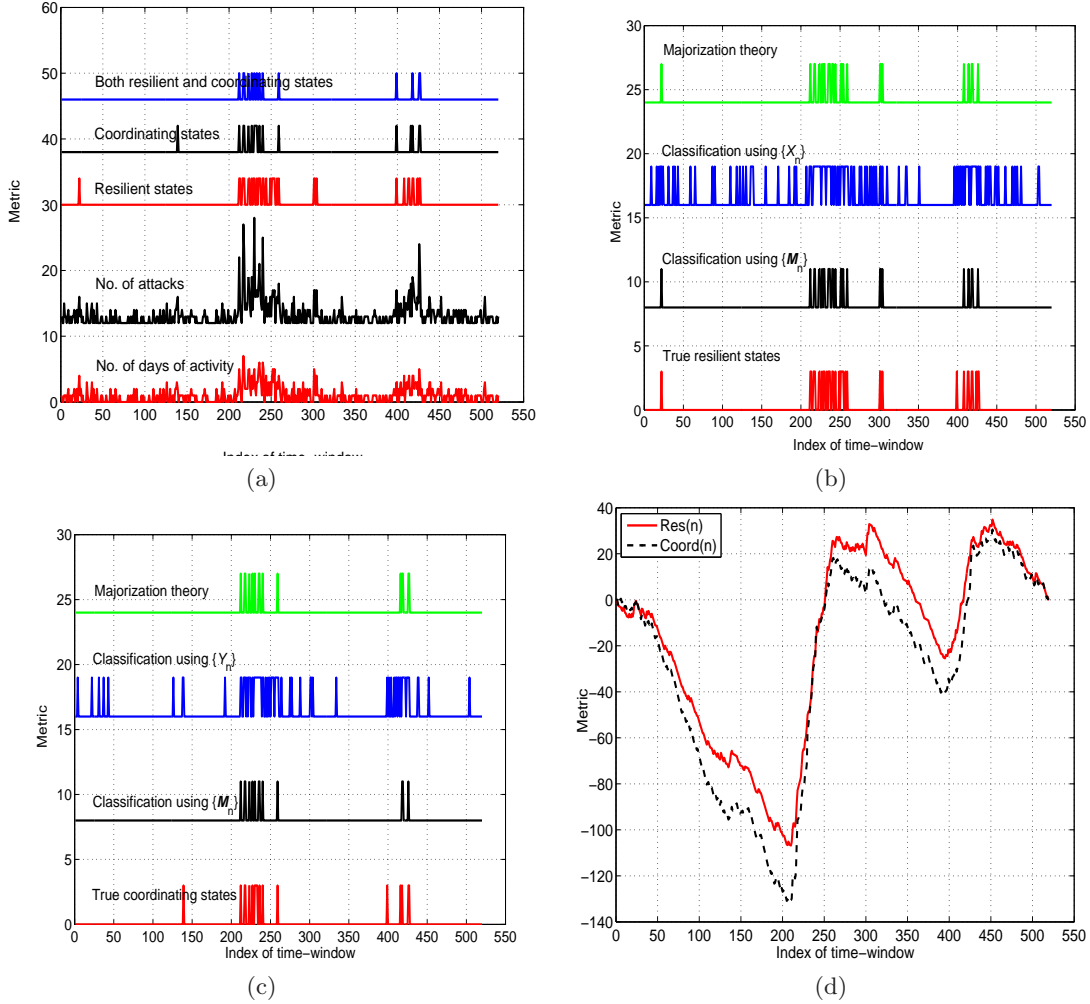


FIG 6. (a) Number of days of activity, number of attacks, and true states of FARC, (b) Resilient and (c) Coordinating state classification with different algorithms, and (d) Resilience and coordination tracking functions over the time-period of interest.

We proceed via the same approach elucidated by [Bilmes \(1998\)](#) leading to

$$\frac{Q(\boldsymbol{\lambda}, \bar{\boldsymbol{\lambda}})}{P(\mathcal{O}|\bar{\boldsymbol{\lambda}})} = \frac{\sum_{n=1}^N \sum_{S_0} \log \left(P(S_0|\boldsymbol{\lambda}) \right) \cdot P(\mathcal{O}, S_0|\bar{\boldsymbol{\lambda}})}{P(\mathcal{O}|\bar{\boldsymbol{\lambda}})} + \frac{\sum_{n=1}^N \sum_{S_n, S_{n-1}} \log \left(P(O_n, S_n|S_{n-1}, \boldsymbol{\lambda}) \right) \cdot P(\mathcal{O}, S_n, S_{n-1}|\bar{\boldsymbol{\lambda}})}{P(\mathcal{O}|\bar{\boldsymbol{\lambda}})}.$$

The component of the auxiliary function corresponding to the initial probability parameters

can be written as:

$$\frac{Q(\boldsymbol{\lambda}, \bar{\boldsymbol{\lambda}}) \Big|_{\text{Init. probability}}}{P(\mathcal{O}|\bar{\boldsymbol{\lambda}})} = \sum_{j=0}^1 \log(\pi_j) \cdot \underbrace{P(S_0 = j|\mathcal{O}, \bar{\boldsymbol{\lambda}})}_{\triangleq \gamma_0(j)},$$

where the iterative update for $\gamma_0(j)$ follows from the forward and backward algorithms (see [Rabiner \(1989, Sec. IIIA and B\)](#)). It can be easily seen that

$$\hat{\pi}_j = \frac{\gamma_0(j)}{\sum_{k=0}^1 \gamma_0(k)}.$$

Similarly, the component of the auxiliary function corresponding to the transition probability parameters can be written as:

$$\begin{aligned} & \frac{Q(\boldsymbol{\lambda}, \bar{\boldsymbol{\lambda}}) \Big|_{\text{Trans. probability}}}{P(\mathcal{O}|\bar{\boldsymbol{\lambda}})} \\ &= \sum_{n=1}^N \sum_{i=0}^1 \sum_{j=0}^1 \log \left(P(S_n = j|S_{n-1} = i, \boldsymbol{\lambda}) \right) \cdot \underbrace{P(S_n = j, S_{n-1} = i|\mathcal{O}, \bar{\boldsymbol{\lambda}})}_{\triangleq \zeta_{n-1}(i,j)}, \end{aligned}$$

where the iterative update for $\zeta_{n-1}(i, j)$ follows from [Rabiner \(1989, Sec. IIIC\)](#). A simple constrained optimization problem results in

$$\begin{aligned} \hat{\mathbf{p}}_0 &= \frac{\sum_{n=1}^N \zeta_{n-1}(0, 1)}{\sum_{n=1}^N \sum_{j=0}^1 \zeta_{n-1}(0, j)}, \\ \hat{\mathbf{q}}_0 &= \frac{\sum_{n=1}^N \zeta_{n-1}(1, 0)}{\sum_{n=1}^N \sum_{j=0}^1 \zeta_{n-1}(1, j)}. \end{aligned}$$

On the other hand, the component of the auxiliary function corresponding to the optimization of observation density parameters can be expressed as:

$$\frac{Q(\boldsymbol{\lambda}, \bar{\boldsymbol{\lambda}}) \Big|_{\text{Obs. density}}}{P(\mathcal{O}|\bar{\boldsymbol{\lambda}})} = \sum_{n=1}^N \sum_{j=0}^1 \log \left(P(O_n|S_n = j, \boldsymbol{\lambda}) \right) \cdot \underbrace{P(S_n = j|\mathcal{O}, \bar{\boldsymbol{\lambda}})}_{\triangleq \gamma_n(j)},$$

where the iterative update for $\gamma_n(j)$ also follows from the forward and backward algorithms (see [Rabiner, 1989, Sec. IIIA and B](#)). We now develop update equations for γ_j and μ_j , specialized based on the observations in the HMM.

7. $\{M_i\}$ as Observations. With $\mathcal{O} = \{M_i\}$, using the hurdle-based geometric model, it is straightforward to check the following update equations for $\hat{\gamma}_j$ and $\hat{\mu}_j$:

$$\begin{aligned}\hat{\gamma}_j &= \frac{\sum_{n=1}^N \mathbb{1}(M_n > 0) \cdot \gamma_n(j)}{\sum_{n=1}^N \gamma_n(j)}, \\ \hat{\mu}_j &= \frac{\sum_{n=1}^N (M_n - 1) \cdot \mathbb{1}(M_n > 0) \cdot \gamma_n(j)}{\sum_{n=1}^N M_n \cdot \mathbb{1}(M_n > 0) \cdot \gamma_n(j)}.\end{aligned}$$

By definition, it is clear that $0 \leq \{\hat{\gamma}_j, \hat{\mu}_j\} \leq 1$.

8. Associating State Changes with *Tactics* in Inferencing with $\{M_i\}$. The proposed approach in Sec. 3.1 of the main paper requires a mapping of the state estimates $\hat{\mathbf{S}}_i|_{i \in \Delta_n}$ to appropriate resilience and/or coordination metric(s). We now provide details on the specific choices of $f(\cdot)$ and $g(\cdot)$ in (3.2) of the main paper to associate state changes with specific changes in *Tactics*.

Motivated by the discussion on resilience and coordination, we propose the following mappings for inferencing corresponding to certain choices of $\hat{\eta}$, $\hat{\eta}_X$ and $\hat{\eta}_Y$:

$$(8.1) \quad \sum_{i \in \Delta_n} \hat{\mathbf{S}}_i > \hat{\eta} \text{ and } X_n > \hat{\eta}_X \iff \text{Group is resilient in } \Delta_n$$

$$(8.2) \quad \sum_{i \in \Delta_n} \hat{\mathbf{S}}_i > \hat{\eta} \text{ and } Y_n > \hat{\eta}_Y \iff \text{Group is coordinating in } \Delta_n$$

$$(8.3) \quad \sum_{i \in \Delta_n} \hat{\mathbf{S}}_i > \hat{\eta}, X_n > \hat{\eta}_X \text{ and } Y_n > \hat{\eta}_Y \iff \text{Group is resilient \& coordinating in } \Delta_n$$

$$(8.4) \quad \sum_{i \in \Delta_n} \hat{\mathbf{S}}_i > \hat{\eta} \iff \text{Group is Active in } \Delta_n.$$

9. $\{(X_n, Y_n)\}$ as Observations. With the joint sequence

$$\mathcal{O} = \{(X_n, Y_n), n = 1, \dots, K\}$$

as observations, using the density function

$$\begin{aligned}P(X_n = k, Y_n = r | \mathbf{S}_i|_{i \in \Delta_n} = j) \\ = \binom{\delta}{k} \binom{r-1}{r-k} \cdot (1 - \gamma_j)^{\delta-k} (\gamma_j)^k \cdot (1 - \mu_j)^k (\mu_j)^{r-k}, \quad r \geq k,\end{aligned}$$

we have

$$(9.1) \quad \hat{\gamma}_j = \frac{\sum_{n=1}^K X_n \gamma_n(j)}{\delta \cdot \sum_{n=1}^N \gamma_n(j)},$$

$$(9.2) \quad \hat{\mu}_j = \frac{\sum_{n=1}^K (Y_n - X_n) \gamma_n(j)}{\sum_{n=1}^N Y_n \gamma_n(j)} = 1 - \frac{\sum_{n=1}^K X_n \gamma_n(j)}{\sum_{n=1}^N Y_n \gamma_n(j)}.$$

The expressions for $\hat{\gamma}_j$ and $\hat{\mu}_j$ have also been derived by [Raghavan, Galstyan and Tartakovsky \(2013\)](#). Note that $X_n \in [0, \delta]$ and $X_n \leq Y_n$ which imply that $0 \leq \{\hat{\gamma}_j, \hat{\mu}_j\} \leq 1$.

10. $\{X_n\}$ as Observations. With $\mathcal{O} = \{X_n, n = 1, \dots, K\}$, using the binomial density function, we have

$$(10.1) \quad \hat{\gamma}_j = \frac{\sum_{n=1}^K X_n \gamma_n(j)}{\delta \cdot \sum_{n=1}^K \gamma_n(j)}.$$

Note that the update equation (10.1) has the same structure as the corresponding expression in (9.1). However, the difference between the two cases is that the update equation for $\gamma_n(j)$ depends on the choice of \mathcal{O} and the associated density functions.

On the other hand, since $\{X_n\}$ does not allow inferencing on μ_j , we recall the facts that

$$\begin{aligned} \mathbb{E}[\mathbf{M}_i | \mathcal{H}_j] &= \frac{\gamma_j}{1 - \mu_j} \\ \text{Var}(\mathbf{M}_i | \mathcal{H}_j) &= \frac{\gamma_j \cdot (1 + \mu_j - \gamma_j)}{(1 - \mu_j)^2}, \end{aligned}$$

which allows μ_j to be rewritten as

$$\mu_j = \frac{\text{Var}(\mathbf{M}_i | \mathcal{H}_j) + \left(\mathbb{E}[\mathbf{M}_i | \mathcal{H}_j]\right)^2 - \mathbb{E}[\mathbf{M}_i | \mathcal{H}_j]}{\text{Var}(\mathbf{M}_i | \mathcal{H}_j) + \left(\mathbb{E}[\mathbf{M}_i | \mathcal{H}_j]\right)^2 + \mathbb{E}[\mathbf{M}_i | \mathcal{H}_j]}.$$

To allow for simple inferencing, we supplant $\hat{\mu}_j$ (for both $j = 0, 1$) with the sample estimate of μ_j using all of $\{\mathbf{M}_i\}$ (implicitly ignoring the two-state HMM framework):

$$(10.2) \quad \hat{\mu}_j = \frac{\sum_{i=1}^N \mathbf{M}_i (\mathbf{M}_i - 1)}{\sum_{i=1}^N \mathbf{M}_i (\mathbf{M}_i + 1)}.$$

It can be seen that $\hat{\mu}_j$ in (10.2) can be approximated as

$$\begin{aligned} \hat{\mu}_j &= \frac{\sum_{n=1}^K \sum_{i \in \Delta_n} \mathbf{M}_i (\mathbf{M}_i - 1)}{\sum_{n=1}^K \sum_{i \in \Delta_n} \mathbf{M}_i (\mathbf{M}_i + 1)} \\ &\stackrel{(a)}{\approx} \frac{\sum_{n=1}^K \sum_{i \in \Delta_n} \mathbf{M}_i \cdot \sum_{i \in \Delta_n} (\mathbf{M}_i - 1)}{\sum_{n=1}^K \sum_{i \in \Delta_n} \mathbf{M}_i \cdot \sum_{i \in \Delta_n} (\mathbf{M}_i + 1)} \\ &\stackrel{(b)}{\approx} \frac{\sum_{n=1}^K \sum_{i \in \Delta_n} \mathbf{M}_i \cdot \sum_{i \in \Delta_n} (\mathbf{M}_i - \mathbb{1}(\mathbf{M}_i > 0))}{\sum_{n=1}^K \sum_{i \in \Delta_n} \mathbf{M}_i \cdot \sum_{i \in \Delta_n} \mathbf{M}_i} \\ &= \frac{\sum_{n=1}^K Y_n \cdot (Y_n - X_n)}{\sum_{n=1}^K Y_n^2} \\ &= 1 - \frac{\sum_{n=1}^K Y_n \cdot X_n}{\sum_{n=1}^K Y_n^2} \end{aligned}$$

where the approximation in (a) assumes that $\sum_k a_k b_k \approx \beta \cdot \sum_k a_k \cdot \sum_k b_k$ for an appropriate choice of β , and the approximation in (b) replaces 1 with $\mathbb{1}(\mathbf{M}_i > 0)$ in the numerator and

discards this factor in the denominator. From the above series of expressions, it can be seen that the expression for $\hat{\mu}_j$ in (10.2) approximates (9.2) with Y_n capturing $\gamma_n(j)$ (in both states) up to a scaling factor. Also, note that $\hat{\mu}_j$ is not an iterative expression depending on the data. It is also important to note that the price to pay for a lack of estimate of μ_j from $\{X_n\}$ is to use $\{Y_n\}$ for it in a non-iterative sense.

11. $\{Y_n\}$ as Observations. With $\mathcal{O} = \{Y_n, n = 1, \dots, K\}$, we now obtain simplified expressions for $\hat{\gamma}_j$ and $\hat{\mu}_j$ under the assumptions that $\delta \gg 1$ and $\mu_j > \gamma_j > \frac{1}{\delta}$.

Recall that the density function of Y_n is given as

$$\mathbb{P}\left(Y_n = r \mid \mathcal{S}_i|_{i \in \Delta_n} = j\right) = (1 - \gamma_j)^\delta \cdot (\mu_j)^r \cdot \sum_{k=1}^{\min(r, \delta)} \binom{\delta}{k} \binom{r-1}{r-k} \cdot \mathbf{A}^k$$

with $\mathbf{A} = \frac{(1-\mu_j)\gamma_j}{(1-\gamma_j)\mu_j}$. Using the moment generating function of a hypergeometric distribution⁷ with parameters (N_1, K_1, n_1) where $N_1 = \delta + r, K_1 = \delta, n_1 = r$, we have

$$(11.1) \quad \sum_{k=0}^{\min(r, \delta)} \binom{\delta}{k} \binom{r}{r-k} \cdot \mathbf{A}^k = {}_2F_1(-r, -\delta; 1; \mathbf{A}),$$

with ${}_2F_1(a, b; c; z)$ denoting the Gauss hypergeometric function (see the definition of this function in Abramowitz and Stegun (1972, 15.1.1, p. 556)). Note that the right-hand side of (11.1) is well-defined as a power series since $\mu_j > \gamma_j$ which implies that $\mathbf{A} < 1$ (and hence within the radius of convergence). Similarly, with $N_1 = r + \delta - 1, K_1 = \delta, n_1 = r - 1$, we have

$$(11.2) \quad \sum_{k=0}^{\min(r-1, \delta)} \binom{\delta}{k} \binom{r-1}{r-1-k} \cdot \mathbf{A}^k = {}_2F_1(-(r-1), -\delta; 1; \mathbf{A}).$$

Combining (11.1) and (11.2), we have

$$\begin{aligned} \frac{\mathbb{P}\left(Y_n = r \mid \mathcal{S}_i|_{i \in \Delta_n} = j\right)}{(1 - \gamma_j)^\delta \cdot (\mu_j)^r} &= {}_2F_1(-r, -\delta; 1; \mathbf{A}) - {}_2F_1(-(r-1), -\delta; 1; \mathbf{A}) \\ &\stackrel{(c)}{=} \delta \mathbf{A} \cdot {}_2F_1(-(r-1), -(\delta-1); 2; \mathbf{A}) \end{aligned}$$

where (c) follows from a straightforward application of the definition of the hypergeometric function that allows the following simplification:

$${}_2F_1(a+1, b; c; z) - {}_2F_1(a, b; c; z) = \frac{bz}{c} \cdot {}_2F_1(a+1, b+1; c+1; z).$$

⁷A hypergeometric distribution with parameters (N_1, K_1, n_1) captures the number of successes in n_1 trials of an experiment from a population of size N_1 with K_1 elements of one type and $N_1 - K_1$ of another type.

Plugging in the expression for the density function of Y_n in the auxiliary function, we have

$$\frac{Q(\boldsymbol{\lambda}, \bar{\boldsymbol{\lambda}}) \Big|_{\text{Obs. density}}}{P(\mathcal{O}|\bar{\boldsymbol{\lambda}})} = \sum_{n=1}^K \sum_{j=0}^1 \left[\delta \log(1 - \gamma_j) + Y_n \log(\mu_j) + \log(\delta) + \log(\mathbf{A}) \right. \\ \left. + \log \left({}_2F_1(-Y_n - 1, -(\delta - 1); 2; \mathbf{A}) \right) \right] \cdot \gamma_n(j).$$

Setting the derivative of the auxiliary function (with respect to γ_j) to zero, we have

$$\begin{aligned} & \frac{\delta \sum_{n=1}^K \gamma_n(j)}{1 - \gamma_j} \\ &= \frac{d\mathbf{A}}{d\gamma_j} \cdot \left[\frac{\sum_{n=1}^K \gamma_n(j)}{\mathbf{A}} + \sum_{n=1}^K \frac{\gamma_n(j) \cdot \frac{d}{d\mathbf{A}} {}_2F_1(-Y_n - 1, -(\delta - 1); 2; \mathbf{A})}{{}_2F_1(-Y_n - 1, -(\delta - 1); 2; \mathbf{A})} \right] \\ &\stackrel{(d)}{=} \frac{d\mathbf{A}}{d\gamma_j} \cdot \left[\frac{\sum_{n=1}^K \gamma_n(j)}{\mathbf{A}} + \sum_{n=1}^K \frac{\gamma_n(j) \cdot {}_2F_1(-Y_n - 2, -(\delta - 2); 3; \mathbf{A})}{{}_2F_1(-Y_n - 1, -(\delta - 1); 2; \mathbf{A})} \right] \\ (11.3) \quad &\stackrel{(e)}{=} \frac{d\mathbf{A}}{d\gamma_j} \cdot \left[\frac{\sum_{n=1}^K \gamma_n(j)}{\mathbf{A}} + \frac{1}{1 - \mathbf{A}} \cdot \sum_{n=1}^K \frac{\gamma_n(j) \cdot {}_2F_1(Y_n + 1, \delta + 1; 3; \mathbf{A})}{{}_2F_1(Y_n + 1, \delta + 1; 2; \mathbf{A})} \right] \end{aligned}$$

where (d) follows from the fact in [Abramowitz and Stegun \(1972, 15.2.1, p. 557\)](#) that

$$\frac{d}{dz} {}_2F_1(a, b; c; z) = \frac{ab}{c} \cdot {}_2F_1(a + 1, b + 1; c + 1; z), \quad z < 1$$

and (e) from the fact in [Abramowitz and Stegun \(1972, 15.3.3, p. 559\)](#) that

$${}_2F_1(a, b; c; z) = (1 - z)^{c-a-b} \cdot {}_2F_1(c - a, c - b; c; z), \quad z < 1.$$

Similarly, setting the derivative of the auxiliary function (with respect to μ_j) to zero, we have

$$(11.4) \quad \frac{\sum_{n=1}^K Y_n \gamma_n(j)}{\mu_j} = -\frac{d\mathbf{A}}{d\mu_j} \cdot \left[\frac{\sum_{n=1}^K \gamma_n(j)}{\mathbf{A}} + \frac{1}{1 - \mathbf{A}} \cdot \sum_{n=1}^K \frac{\gamma_n(j) \cdot {}_2F_1(Y_n + 1, \delta + 1; 3; \mathbf{A})}{{}_2F_1(Y_n + 1, \delta + 1; 2; \mathbf{A})} \right].$$

From the two derivative expressions in (11.3) and (11.4), we clearly have

$$(11.5) \quad \mu_j = 1 - \frac{\gamma_j \cdot \delta \cdot \sum_{n=1}^K \gamma_n(j)}{\sum_{n=1}^K Y_n \gamma_n(j)}.$$

We now simplify the expressions for γ_j and μ_j under the assumptions that $\delta \gg 1$ and $\gamma_j > \frac{1}{\delta}$. For this⁸, we use the following fact from [Magnus, Oberhettinger and Tricomi \(1953, 2.3.2\(13\), p. 77\)](#)

$$\begin{aligned} {}_2F_1(a, b; c; z) &\stackrel{|b| \gg 1}{\sim} {}_1F_1(a; c; bz) \cdot [1 + O(|b|^{-1})] \\ &\stackrel{|b| \gg 1}{\sim} \frac{\Gamma(c)e^{bz}(bz)^{a-c}}{\Gamma(a)} \cdot \left[1 + \frac{1-a}{bz} + \frac{(1-a)(2-a)(c-a)(c-a+1)}{2b^2z^2} \right] \end{aligned}$$

where ${}_1F_1(\cdot; \cdot; \cdot)$ is the confluent hypergeometric function of the first kind (see the definition in [Abramowitz and Stegun \(1972, 13.1.2, p. 505\)](#)) and the second step follows from [MacDonald \(1948, Sec. 4, \(9\)-\(11\)\)](#). Applying these facts to (11.3), we have

$$\frac{{}_2F_1(Y_n + 1, \delta + 1; 3; A)}{{}_2F_1(Y_n + 1, \delta + 1; 2; A)} \stackrel{\delta \gg 1}{\sim} \frac{2}{(\delta + 1)A} \cdot \left[1 + O\left(\frac{1}{\delta}\right) \right]$$

and thus

$$\begin{aligned} \frac{\delta \cdot \sum_{n=1}^K \gamma_n(j)}{1 - \gamma_j} &\stackrel{\delta \gg 1}{\sim} \frac{dA}{d\gamma_j} \cdot \sum_{n=1}^K \gamma_n(j) \cdot \left[\frac{1}{A} + \frac{2}{(1-A)A(\delta+1)} \right] \\ \implies \mu_j &\stackrel{\delta \gg 1}{\sim} \frac{\gamma_j(\delta+1)(\delta\gamma_j-1)}{(\delta+1)(\delta\gamma_j-1) - 2(1-\gamma_j)} \\ (11.6) \quad &= \frac{\gamma_j}{1 - \frac{2(1-\gamma_j)}{(\delta\gamma_j-1)(\delta+1)}}, \end{aligned}$$

where the condition that $\gamma_j > \frac{1}{\delta}$ ensures that $\mu_j > \gamma_j$.

Combining (11.5) with (11.6), it can be seen that γ_j is a solution to the quadratic equation:

$$\begin{aligned} &\gamma_j^2 \cdot \left[(\delta^2 + \delta + 2)\delta \sum_{n=1}^K \gamma_{n,j} + (\delta^2 + \delta) \sum_{n=1}^K Y_n \gamma_{n,j} \right] \\ &- \gamma_j \cdot \left[\delta(\delta + 3) \sum_{n=1}^K \gamma_{n,j} + (\delta^2 + 2\delta + 3) \sum_{n=1}^K Y_n \gamma_{n,j} \right] + (\delta + 3) \sum_{n=1}^K Y_n \gamma_{n,j} = 0. \end{aligned}$$

⁸We use the notation $f(x) \stackrel{x \gg 1}{\sim} g(x)$ to denote that $\lim_{x \rightarrow \infty} \frac{f(x)}{g(x)} = 1$. Further, we use the notation $\lim_{x \rightarrow a} f(x) = O(g(x))$ if there exists ϵ and M such that $|f(x)| \leq M|g(x)|$ for all x such that $|x - a| < \epsilon$. If a choice of a is not specified, it is implicitly assumed to be $+\infty$.

The two solutions to the above quadratic equation in the $\delta \gg 1$ regime are:

$$\begin{aligned} \text{Solution 1 : } \hat{\gamma}_j &= \frac{1}{\delta} \left(1 + \frac{2}{\delta} \right) + O\left(\frac{1}{\delta^3}\right), \\ \hat{\mu}_j &= 1 - \frac{\sum_{n=1}^K \gamma_{n,j}}{\sum_{n=1}^K Y_n \gamma_{n,j}} \cdot \left(1 + \frac{2}{\delta} \right) + O\left(\frac{1}{\delta^2}\right), \\ \text{Solution 2 : } \hat{\gamma}_j &= \frac{\sum_{n=1}^K Y_n \gamma_{n,j}}{\delta \sum_{n=1}^K \gamma_{n,j}} \cdot \left(1 - \frac{\sum_{n=1}^K Y_n \gamma_{n,j}}{\delta \sum_{n=1}^K \gamma_{n,j}} \right) + O\left(\frac{1}{\delta^3}\right), \\ \hat{\mu}_j &= \frac{\sum_{n=1}^K Y_n \gamma_{n,j}}{\delta \sum_{n=1}^K \gamma_{n,j}} + O\left(\frac{1}{\delta^2}\right). \end{aligned}$$

To ensure that the three conditions ($\hat{\gamma}_j > \frac{1}{\delta}$, $\hat{\mu}_j > \hat{\gamma}_j$ and $\hat{\mu}_j < 1$) are met, we note that **Solution 1** needs to satisfy the condition that $\frac{\sum_{n=1}^K \gamma_{n,j}}{\sum_{n=1}^K Y_n \gamma_{n,j}} < 1 - \frac{1}{\delta}$, whereas **Solution 2** needs to satisfy the condition $\frac{1}{\delta} < \frac{\sum_{n=1}^K \gamma_{n,j}}{\sum_{n=1}^K Y_n \gamma_{n,j}} < 1$. While either condition does not appear to suffer from any technical difficulties in the $\delta \gg 1$ regime, it is clear that **Solution 2** converges to a geometric model ($\gamma_j = \mu_j$) since

$$\frac{\hat{\gamma}_j}{\hat{\mu}_j} \stackrel{\delta \gg 1}{\sim} 1.$$

This solution particularizes the hurdle-based geometric model and thus reduces the general model to a special case. Thus, we use **Solution 1** for the update equations with $\mathcal{O} = \{Y_n\}$ as observations. Note that the structure of **Solution 1** follows the same general structure as (9.1)-(9.2) with $X_n = 1 + \frac{2}{\delta}$. However, as before, the update equation for $\gamma_n(j)$ depends on the choice of \mathcal{O} and the associated density functions.

Supplementary B: Background on majorization theory

(; .pdf). This section provides a brief primer on majorization theory and reverse majorization.

12. Preliminaries. We refer the readers to the seminal book by [Marshall and Olkin \(1979\)](#) for a comprehensive background on majorization theory. Here, we provide a brief review of the main theoretical underpinning needed to develop this paper.

Let \mathbb{P}_δ denote the space of probability vectors of length δ with $\underline{P} = [P(1), \dots, P(\delta)] \in \mathbb{P}_\delta \implies P(i) \geq 0$ for all $i = 1, \dots, \delta$ and $\sum_i P(i) = 1$. Without loss in generality, we can assume that the entries of \underline{P} are arranged in non-increasing order ($P(1) \geq \dots \geq P(\delta)$).

DEFINITION 1 (Majorization). Let $\{\underline{P}, \underline{Q}\} \in \mathbb{P}_\delta$. We say that \underline{P} is majorized by \underline{Q} and denote it as $\underline{P} \prec \underline{Q}$ if

$$(12.1) \quad \sum_{i=1}^k P(i) \leq \sum_{i=1}^k Q(i), \quad k = 1, \dots, \delta.$$

Note that equality holds in (12.1) for $k = \delta$ because $\{\underline{P}, \underline{Q}\} \in \mathbb{P}_\delta$, which implies that $\sum_i P(i) = 1 = \sum_i Q(i)$.

□

The majorization relationship captures the notion that \underline{P} is more well-spread out than \underline{Q} . It also vaguely captures the notion that \underline{P} is more unambiguously random/bursty than \underline{Q} . We now provide many illustrative examples of majorization. In the first example, as k decreases from δ to 1, we have a progressive majorization relationship:

$$\left[\underbrace{1/\delta, \dots, 1/\delta}_{\delta \text{ times}} \right] \prec \dots \prec \left[\underbrace{1/k, \dots, 1/k}_k, \underbrace{0, \dots, 0}_{(\delta-k) \text{ times}} \right] \prec \dots \prec \left[1, \underbrace{0, \dots, 0}_{(\delta-1) \text{ times}} \right].$$

On the other hand, any $\underline{P} \in \mathbb{P}_\delta$ satisfies:

$$\left[\underbrace{1/\delta, \dots, 1/\delta}_{\delta \text{ times}} \right] \prec \underline{P} \prec \left[1, \underbrace{0, \dots, 0}_{(\delta-1) \text{ times}} \right].$$

In this sense, any vector \underline{P} majorizes $\left[\underbrace{1/\delta, \dots, 1/\delta}_{\delta \text{ times}} \right]$ and is majorized by $\left[1, \underbrace{0, \dots, 0}_{(\delta-1) \text{ times}} \right]$.

An easy consequence of the above majorization relationship is that for any $c \geq 0$ and any $\underline{P} \in \mathbb{P}_\delta$, we have

$$\frac{[P(1) + c, \dots, P(\delta) + c]}{1 + \delta c} \prec \underline{P}.$$

In the $\delta = 2$ case, we have

$$(12.2) \quad [P(1), 1 - P(1)] \prec [Q(1), 1 - Q(1)] \iff \frac{1}{2} \leq P(1) \leq Q(1).$$

While a similar set of equivalent inequalities on the entries of \underline{P} and \underline{Q} can be written for the $\delta \geq 3$ case, they quickly get overwhelmingly complicated.

DEFINITION 2 (Schur-convex and -concave functions). *A function $f : (\mathbb{R}^+)^{\delta} \mapsto \mathbb{R}$ is said to be Schur-convex if for any \underline{P} and \underline{Q} with $\underline{P} \prec \underline{Q}$, we have $f(\underline{P}) \leq f(\underline{Q})$. A function $f(\cdot)$ is Schur-concave if $-f(\cdot)$ is Schur-convex. That is, $\underline{P} \prec \underline{Q}$ implies that $f(\underline{P}) \geq f(\underline{Q})$.*

□

We now provide some examples of Schur-convex and Schur-concave functions.

PROPOSITION 1. *The counting function of non-zero elements in \underline{P} (also called the rank function), defined as,*

$$\text{NZ}(\underline{P}) \triangleq \sum_i \mathbb{1}(P(i) > 0)$$

is Schur-concave. If $\mathbf{P}(i) = 0$, let $-\mathbf{P}(i) \log(\mathbf{P}(i))$ be extended continuously to 0 and $\mathbf{P}(i)^\alpha$ be extended continuously to 0 if $\alpha > 0$ and to $+\infty$ if $\alpha < 0$. Then, the Shannon entropy and geometric mean functions, defined respectively as,

$$\text{SE}(\underline{\mathbf{P}}) \triangleq - \sum_i \mathbf{P}(i) \log(\mathbf{P}(i)), \quad \text{GM}(\underline{\mathbf{P}}) \triangleq \left(\prod_i \mathbf{P}(i) \right)^{1/\delta}$$

are also Schur-concave. The power mean function corresponding to an index α , defined as,

$$\text{PM}(\underline{\mathbf{P}}, \alpha) \triangleq \left(\frac{\sum_i \mathbf{P}(i)^\alpha}{\sum_i \mathbb{1}(\mathbf{P}(i) > 0)} \right)^{1/\alpha}$$

is Schur-convex if $\alpha \geq 1$ and Schur-concave if $\alpha \leq 1$, $\alpha \neq 0$.

PROOF. To see that $\text{NZ}(\underline{\mathbf{P}})$ is Schur-concave, assume that $\underline{\mathbf{P}} \prec \underline{\mathbf{Q}}$ and let

$$\underline{\mathbf{Q}} = [\mathbf{Q}(1), \dots, \mathbf{Q}(p), 0, \dots, 0]$$

with $\mathbf{Q}(p) > 0$ for some p . A rewriting of the condition in (12.1) is:

$$(12.3) \quad \sum_{i=k}^{\delta} \mathbf{P}(i) \geq \sum_{i=k}^{\delta} \mathbf{Q}(i), \quad k = 1, \dots, \delta.$$

With $k = p$ in (12.3), we have $\sum_{i=p}^{\delta} \mathbf{P}(i) \geq \mathbf{Q}(p) > 0$. We have a contradiction if $\mathbf{P}(p) = 0$ since $\{\mathbf{P}(p), \dots, \mathbf{P}(\delta)\}$ are arranged in non-increasing order and all of them have to be 0. Thus, $\mathbf{P}(p) > 0$ and this implies that

$$\sum_{i=1}^{\delta} \mathbb{1}(\mathbf{P}(i) > 0) \geq \sum_{i=1}^{\delta} \mathbb{1}(\mathbf{Q}(i) > 0).$$

The proof of the Schur-convexity or -concavity of the different functional structures in the statement of the proposition follow from the main result from Marshall and Olkin (1979, Prop. 3.C.1, p. 64) that if $g : (0, \infty) \mapsto \mathbb{R}$ is convex (or concave), then $\underline{\mathbf{P}} \mapsto \sum_i g(\mathbf{P}(i))$ is Schur-convex (or Schur-concave). In the setting where $\{\underline{\mathbf{P}}, \underline{\mathbf{Q}}\} \in \mathbb{P}_\delta$, but with some zero entries, all the inequality relations corresponding to Schur-convexity and -concavity hold trivially with the appropriate continuous extensions. \square

COROLLARY 1. A straightforward consequence of Prop. 1 is that the normalized power mean, defined as,

$$\text{NPM}(\underline{\mathbf{P}}, \alpha) \triangleq \frac{\text{PM}(\underline{\mathbf{P}}, \alpha)}{\text{NZ}(\underline{\mathbf{P}})}$$

is Schur-convex if $\alpha > 1$. Note that Schur-concavity of the normalized power mean may not hold if $\alpha < 1$ except in the trivial case where $\text{NZ}(\underline{\mathbf{P}}) = \text{NZ}(\underline{\mathbf{Q}})$.

□

From the example in (12.2), it is clear that majorization theory provides a complete ordering (all vectors are comparable with each other) in the $\delta = 2$ case. However, for $\delta \geq 3$, it is important to observe that majorization theory provides only a partial ordering. For example, it can be seen that both $\underline{P} \not\prec \underline{Q}$ and $\underline{Q} \not\prec \underline{P}$ are true with the choice $\underline{P} = [0.5, 0.25, 0.25]$ and $\underline{Q} = [0.4, 0.4, 0.2]$. Another such choice with $\delta = 4$ is $\underline{P} = [0.4, 0.35, 0.15, 0.1]$ and $\underline{Q} = [0.45, 0.27, 0.25, 0.03]$. Thus, two arbitrary probability vectors in \mathbb{P}_δ cannot necessarily be compared by a majorization relationship. Further, while Schur-convexity and -concavity allow an ordering of vectors from \mathbb{P}_δ to \mathbb{R} , we seek a reverse majorization theory where $f(\underline{P}) \leq f(\underline{Q})$ for an appropriate choice of $f(\cdot)$ implies that $\underline{P} \prec \underline{Q}$.

13. Reverse Majorization. The notion of reverse majorization is established over a bigger subset of \mathbb{P}_δ by extending (or “lifting”) the majorization relationship to that of *catalytic majorization*. The idea was first proposed by [Jonathan and Plenio \(1999\)](#) in the context of quantum entanglement. Various terms such as *trumping*, *entanglement catalysis*, *entanglement-assisted local transformation*, etc., are used in the literature to describe it.

DEFINITION 3 (Catalytic majorization). *Let $\{\underline{P}, \underline{Q}\} \in \mathbb{P}_\delta$. We say that \underline{P} is catalytically majorized by \underline{Q} if there exists some $m \geq 1$ and some $\underline{L} \in \mathbb{P}_m$ such that*

$$(13.1) \quad \underline{P} \otimes \underline{L} \prec \underline{Q} \otimes \underline{L},$$

where \otimes denotes the Kronecker product operation:

$$\underline{P} \otimes \underline{L} \triangleq [P(1)L(1), \dots, P(1)L(m), P(2)L(1), \dots, P(2)L(m), \dots, P(\delta)L(1), \dots, P(\delta)L(m)].$$

Note that without loss in generality, \underline{L} can be assumed to satisfy $L(m) > 0$.

□

Technically speaking, catalytic majorization is tensor product-induced majorization, where \underline{L} can be seen as a “resource that allows one to transform \underline{P} (a certain state) into \underline{Q} (another state) via local operations and classical information; this vector \underline{L} remains unaltered after being used, yet the transformation could not occur without its presence” (the above explanation is sourced *verbatim* from ([Plosker, 2013](#), p. 113)). The distinction between majorization and catalytic majorization comes from the fact that while most majorization results hold even if the components of the vectors are negative, almost all of the catalytic majorization results critically depend on the non-negativity of the vector components. Note that the δm inequality relations corresponding to (12.1) need to be checked to verify $\underline{P} \otimes \underline{L} \prec \underline{Q} \otimes \underline{L}$ after reordering the entries of $\underline{P} \otimes \underline{L}$ and $\underline{Q} \otimes \underline{L}$ in non-increasing order. Further, no specific conditions are imposed on the length m of \underline{L} nor on the uniqueness of \underline{L} . Without reference to \underline{L} , we denote the relationship in (13.1) as $\underline{P} \prec_T \underline{Q}$, with T standing for “trumping.”

The following result shows that \prec_T is also not a complete ordering on \mathbb{P}_δ . Nevertheless, the set of vectors that can be catalytically majorized is strictly larger than the set that can be majorized.

PROPOSITION 2. (a) *Clearly, if $\underline{P} \prec \underline{Q}$, then $\underline{P} \prec_T \underline{Q}$ since $m = 1$ and $\underline{L} = [1]$ can be used to establish catalytic majorization. But more generally, $\underline{P} \prec \underline{Q}$ implies that $\underline{P} \prec_T \underline{Q}$ for any choice of m and for any $\underline{L} \in \mathbb{P}_m$.*

(b) *In converse, if $\underline{P} \prec_T \underline{Q}$ for some $\underline{L} \in \mathbb{P}_m$ and $\delta \leq 3$, then $\underline{P} \prec \underline{Q}$. In general, if $\delta \geq 4$, there exists an \underline{P} and \underline{Q} such that $\underline{P} \prec_T \underline{Q}$, but $\underline{P} \not\prec \underline{Q}$. In the $\delta \geq 4$ case, the set of vectors majorized by \underline{Q} is a strict subset of the set of vectors catalytically majorized by it provided that \underline{Q} has at least four distinct components.*

PROOF. For (a), we first note that given that there is no simple algorithm that captures the order of non-increasing entries of $\underline{P} \otimes \underline{L}$, verifying the δm inequalities of (12.1) is a difficult exercise in general. To overcome this problem, we note that $\underline{P} \prec \underline{Q}$ is equivalent to the fact from Marshall and Olkin (1979, Prop. 4.B.3, p. 109) that $\sum_{i=1}^\delta \mathbf{P}(i) = \sum_{i=1}^\delta \mathbf{Q}(i)$ and $\sum_{i=1}^\delta (\mathbf{P}(i) - t)^+ \leq \sum_{i=1}^\delta (\mathbf{Q}(i) - t)^+$ for all $t \in \mathbb{R}$ where $(x)^+ = \max(x, 0)$ is the positive part function. From this fact, assuming without loss in generality that $\mathbf{L}(m) > 0$, we can easily see that

$$\sum_{i=1}^\delta \sum_{j=1}^m \mathbf{P}(i) \mathbf{L}(j) = \sum_i \mathbf{P}(i) \cdot \sum_j \mathbf{L}(j) = 1 = \sum_i \mathbf{Q}(i) \cdot \sum_j \mathbf{L}(j) = \sum_{i=1}^\delta \sum_{j=1}^m \mathbf{Q}(i) \mathbf{L}(j).$$

Further, for all $t \in \mathbb{R}$, we have

$$\begin{aligned} \sum_{j=1}^m \sum_{i=1}^\delta (\mathbf{P}(i) \mathbf{L}(j) - t)^+ &= \sum_{j=1}^m \mathbf{L}(j) \cdot \sum_{i=1}^\delta \left(\mathbf{P}(i) - \frac{t}{\mathbf{L}(j)} \right)^+ \\ &\stackrel{(a)}{\leq} \sum_{j=1}^m \mathbf{L}(j) \cdot \sum_{i=1}^\delta \left(\mathbf{Q}(i) - \frac{t}{\mathbf{L}(j)} \right)^+ = \sum_{j=1}^m \sum_{i=1}^\delta (\mathbf{Q}(i) \mathbf{L}(j) - t)^+ \end{aligned}$$

where (a) follows from the assumption that $\underline{P} \prec \underline{Q}$. This implies that $\underline{P} \otimes \underline{L} \prec \underline{Q} \otimes \underline{L}$.

For (b), note that catalytic majorization $\underline{P} \prec_T \underline{Q}$ implies that (see Jonathan and Plenio (1999)) $\mathbf{P}(1) \mathbf{L}(1) \leq \mathbf{Q}(1) \mathbf{L}(1)$ (which is equivalent to $\mathbf{P}(1) \leq \mathbf{Q}(1)$) and $\mathbf{P}(\delta) \mathbf{L}(\delta) \geq \mathbf{Q}(\delta) \mathbf{L}(\delta)$ (which is equivalent to $\mathbf{P}(\delta) \geq \mathbf{Q}(\delta)$). If $\delta = 2$, these facts clearly imply that $\frac{1}{2} \leq \mathbf{P}(1) \leq \mathbf{Q}(1)$, which from (12.2) is equivalent to the fact that $\underline{P} \prec \underline{Q}$. If $\delta = 3$, combining $\mathbf{P}(1) \leq \mathbf{Q}(1)$ and $\mathbf{P}(3) \geq \mathbf{Q}(3)$ results in $\underline{P} \prec \underline{Q}$. For the first counterexample in the $\delta \geq 4$ case, while the previous discussion showed that $\underline{P} = [0.4, 0.35, 0.15, 0.1]$ and $\underline{Q} = [0.45, 0.27, 0.25, 0.03]$ result in $\underline{P} \not\prec \underline{Q}$ and $\underline{Q} \not\prec \underline{P}$, we also have that $\underline{P} \otimes \underline{L} \prec \underline{Q} \otimes \underline{L}$ with the choice $\underline{L} = [0.6, 0.4]$. For the second counterexample, the choice $\underline{P} = [0.4, 0.27, 0.27, 0.06]$ and $\underline{Q} = [0.5, 0.2, 0.2, 0.1]$ satisfies $\mathbf{P}(1) \leq \mathbf{Q}(1)$ and $\mathbf{P}(4) < \mathbf{Q}(4)$ and hence, $\underline{P} \not\prec_T \underline{Q}$. The proof of the last statement follows from Theorem 2.4.1 of Daftuar (2004) (also, see Daftuar and Klimesh (2001)). \square

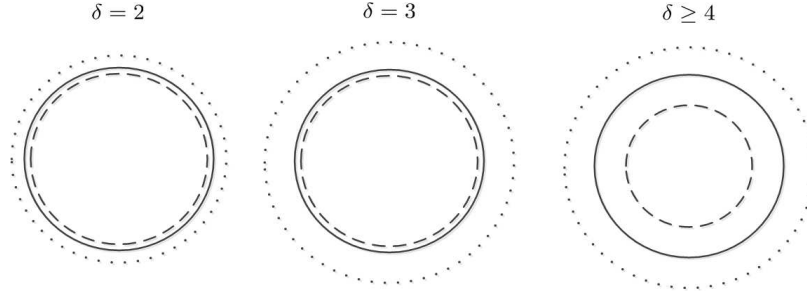


FIG 7. Set inclusion relationships between the set of all vector pairs in \mathbb{P}_δ (denoted by outer circle with dots), the set of all catalytically majorizable vector pairs (denoted by the middle circle with solid lines), and the set of all majorizable vector pairs (denoted by the inner circle with dashed lines).

The conclusions of Prop. 2 in terms of the set inclusion relationships between the set of all vector pairs in \mathbb{P}_δ , the set of all catalytically majorizable vector pairs, and the set of all majorizable vector pairs are pictorially illustrated in Fig. 7 for the $\delta = 2$, $\delta = 3$ and $\delta \geq 4$ cases. The main result from (Turgut, 2007; Klimesh, 2007, 2004) on reverse catalytic majorization is provided next.

THEOREM 2. *Let $\{\underline{P}, \underline{Q}\}$ be distinct elements of \mathbb{P}_δ with $P(\delta) > 0$. We have $\underline{P} \prec_T \underline{Q}$ if and only if all the following conditions hold true:*

- i) $\text{PM}(\underline{P}, \alpha) < \text{PM}(\underline{Q}, \alpha)$ if $\alpha > 1$,
- ii) $\text{PM}(\underline{P}, \alpha) > \text{PM}(\underline{Q}, \alpha)$ if $\alpha < 1$,
- iii) $\text{SE}(\underline{P}) > \text{SE}(\underline{Q})$.

□

An alternate near-equivalent characterization of Theorem 2 is provided in the work by Aubrun and Nechita (2008) in terms of ℓ_p norms of infinite-dimensional probability vectors with finitely many non-zero components, and an equivalent characterization based on an alternate approach is provided in terms of general Dirichlet polynomials and Mellin transforms by Pereira and Plosker (2013) and in terms of completely monotone functions by Kribs, Pereira and Plosker (2013).

At this stage, it is important to note that

$$\begin{aligned} \lim_{\alpha \rightarrow \infty} \text{PM}(\underline{P}, \alpha) &= \max_{i=1, \dots, \delta} P(i), \\ \lim_{\alpha \rightarrow -\infty} \text{PM}(\underline{P}, \alpha) &= \min_{i=1, \dots, \delta} P(i), \text{ and} \\ \lim_{\alpha \rightarrow 0} \text{PM}(\underline{P}, \alpha) &= \text{GM}(\underline{P}). \end{aligned}$$

While we know from the proof of Prop. 2 that $\max_{i=1, \dots, \delta} P(i) \leq \max_{i=1, \dots, \delta} Q(i)$ and $\min_{i=1, \dots, \delta} P(i) \geq \min_{i=1, \dots, \delta} Q(i)$ when $\underline{P} \prec_T \underline{Q}$. Theorem 2 is along the right direction

in the limiting settings of $\alpha \rightarrow \infty$ and $\alpha \rightarrow -\infty$ except for the modification of the strict inequality with an inclusive inequality in these cases. Further, while the statement of Theorem 2 has not made any assumption on whether $\mathbf{Q}(\delta) > 0$ or $\mathbf{Q}(\delta) = 0$, it is clear that the inequalities hold in the latter case since

$$\text{PM}(\underline{\mathbf{P}}, \alpha) = 0 \quad \text{if } \alpha \leq 0,$$

with the equality seen as a limiting case of $\alpha \rightarrow 0^-$ at the extreme point.

The importance of Theorem 2 is in emphasizing the role of *only* two specific candidate functionals (Shannon entropy and power mean) from a broad class of functionals that might have potentially been of importance. For example $\text{NZ}(\underline{\mathbf{P}})$ is a Schur-concave function that is not important from the viewpoint of catalytic majorization. However, while Theorem 2 characterizes catalytic majorization in terms of two functions, it is imperative to note that they correspond to an *uncountably* infinite set of inequalities in the parameter α . It is widely conjectured by Klimesh (2007, 2004) that a significant computational reduction in this checking might not be possible. Nevertheless, in the following special case, the checking of the infinitely many power mean functions is not necessary and only the Shannon entropy function is seen to be important.

PROPOSITION 3. *Let $\{\underline{\mathbf{P}}, \underline{\mathbf{Q}}\} \in \mathbb{P}_\delta$ with $\mathbf{P}(k^*) > 0$ where $k^* = \arg \max_{k=1, \dots, \delta} \{\mathbf{Q}(k) > 0\}$.
If*

$$\frac{\mathbf{Q}(1)}{\mathbf{P}(1)} \geq \dots \geq \frac{\mathbf{Q}(k^*)}{\mathbf{P}(k^*)},$$

then

$$\begin{aligned} \text{PM}(\underline{\mathbf{P}}, \alpha) &< \text{PM}(\underline{\mathbf{Q}}, \alpha), \quad \text{if } \alpha > 1 \text{ and} \\ \text{PM}(\underline{\mathbf{P}}, \alpha) &> \text{PM}(\underline{\mathbf{Q}}, \alpha), \quad \text{if } \alpha > 1. \end{aligned}$$

PROOF. The proof follows from the monotonicity of ratio of means in the α parameter (Marshall and Olkin, 1979, Prop. 5.B.3, p. 130) under the assumptions made in the statement of the proposition and by comparing it with the $\alpha = 1$ case where the ratio of the means of $\underline{\mathbf{P}}$ and $\underline{\mathbf{Q}}$ is 1. \square

References.

- ABRAMOWITZ, M. and STEGUN, I. A. (1972). *Handbook of Mathematical Functions with Formulas, Graphs and Mathematical Tables*, 10th ed. National Bureau of Standards, USA.
- AUBRUN, G. and NECHITA, I. (2008). Catalytic majorization and ℓ_p norms. *Communications in Mathematical Physics* **278** 133-144.
- BAKKER, R. M., RAAB, J. and MILWARD, H. B. (2012). A preliminary theory of dark network resilience. *Journal of Policy Analysis and Management* **31** 33-62.
- BASSEVILLE, M. and NIKIFOROV, I. V. (1993). *Detection of Abrupt Changes: Theory and Applications*. Prentice Hall, Englewood Cliffs, NJ.
- BILMES, J. A. (1998). A gentle tutorial of the EM algorithm and its application to parameter estimation for Gaussian mixture and hidden Markov models, Technical Report, International Computer Science Institute, Berkeley, CA.

- BLOMBERG, B. S., GAIBULLOEV, K. and SANDLER, T. (2011). Terrorist group survival: Ideology, tactics, and base of operations. *Public Choice* **149** 441-463.
- BREIGER, R. L., ACKERMAN, G. A., ASAL, V., MELAMED, D., MILWARD, H. B., RETHEMEYER, R. K. and SCHOON, E. (2011). Application of a profile similarity methodology for identifying terrorist groups that use or pursue CBRN weapons. In *J. Salerno, S. J. Yang, D. Nau, S.-K. Chai (Eds.), Social Computing, Behavioral-Cultural Modeling, and Prediction. Springer (Lecture Notes in Computer Science 6589)* 26-33.
- CAULEY, J. and IM, E. I. (1988). Intervention policy analysis of skyjackings and other terrorist incidents. *The American Economic Review* **78** 27-31.
- CRAGIN, K. and DALY, S. A. (2004). *The Dynamic Terrorist Threat: An Assessment of Group Motivations and Capabilities in a Changing World*. RAND Corporation, Santa Monica, CA.
- DAFTUAR, S. K. (2004). Eigenvalue inequalities in quantum information processing, Technical Report, California Institute of Technology. Ph.D. dissertation.
- DAFTUAR, S. and KLIMESH, M. (2001). Mathematical structure of entanglement catalysis. *Physics Review A* **64**.
- DUGAN, L., LAFREE, G. and PIQUERO, A. (2005). Testing a rational choice model of airline hijackings. *Criminology* **43** 1031-1065.
- ENDERS, W. and SANDLER, T. (1993). The effectiveness of antiterrorism policies: A vector autoregression-intervention analysis. *The American Political Science Review* **87** 829-844.
- ENDERS, W. and SANDLER, T. (2000). Is transnational terrorism becoming more threatening? A time-series investigation. *Journal of Conflict Resolution* **44** 307-332.
- GIBBONS, J. D. and CHAKRABORTI, S. (2011). *Nonparametric Statistical Inference*, 5th ed. CRC Press.
- HAWKES, A. G. (1971). Spectra of some self-exciting and mutually exciting point processes. *Biometrika* **58** 83-90.
- JONATHAN, D. and PLENIO, M. B. (1999). Entanglement-assisted local manipulation of pure quantum states. *Physics Review Letters* **83** 3566-3569.
- KLIMESH, M. (2004). Entropy measures and catalysis of bipartite quantum state transformations. *Proc. IEEE International Symposium on Information Theory, Chicago, IL* 357.
- KLIMESH, M. (2007). Inequalities that collectively completely characterize the catalytic majorization relation. Available: [Online]. <http://arxiv.org/abs/0709.3680v1>.
- KRIBS, D. W., PEREIRA, R. and PLOSKER, S. (2013). Trumping and power majorization. *Linear and Multilinear Algebra* **61** 1455-1463.
- LAFREE, G. and DUGAN, L. (2007). Introducing the Global Terrorism Database. *Terrorism and Political Violence* **19** 181-204.
- LAFREE, G., MORRIS, N. A. and DUGAN, L. (2010). Cross-national patterns of terrorism, comparing trajectories for total, attributed and fatal attacks, 1970-2006. *British Journal of Criminology* **50** 622-649.
- LANDES, W. M. (1978). An economic study of U.S. aircraft hijackings, 1961-1976. *Journal of Law and Economics* **21** 1-31.
- LINDBERG, M. (2010). Factors contributing to the strength and resilience of terrorist groups. *Grupo de Estudios Estrategicos (GEES) Publication*.
- MACDONALD, A. D. (1948). Properties of the confluent hypergeometric function, Technical Report, Massachusetts Institute of Technology. No. 84.
- MAGNUS, W., OBERHETTINGER, F. and TRICOMI, F. G. (1953). *Higher Transcendental Functions, Vol. 1*. McGraw Hill Book Company, New York.
- MARSHALL, A. W. and OLKIN, I. (1979). *Inequalities: Theory of Majorization and its Applications*. Academic Press, NY.
- MELAMED, D., SCHOON, E., BREIGER, R. L., ASAL, V. and RETHEMEYER, R. K. (2012). Using organizational similarity to identify statistical interactions for improving situational awareness of CBRN activities. In *S. J. Yang, A. M. Greenberg and M. Endsley (Eds.), Social Computing, Behavioral-Cultural Modeling, and Prediction. Springer (Lecture Notes in Computer Science 7227)* 61-68.
- MOHLER, G. O., SHORT, M. B., BRANTINGHAM, P. J., SCHOENBERG, F. P. and TITA, G. E. (2011). Self-exciting point process modeling of crime. *Journal of the American Statistical Association* **106** 100-108.

- PEREIRA, R. and PLOSKER, S. (2013). Dirichlet polynomials, majorization, and trumping. *Journal of Physics A: Mathematical and Theoretical* **46** 225302.
- PLOSKER, S. (2013). Matrix analysis and operator theory with applications to quantum information theory, Technical Report, The University of Guelph, Ontario, Canada. Ph.D. dissertation.
- PORTER, M. D. and WHITE, G. (2012). Self-exciting hurdle models for terrorist activity. *Annals of Applied Statistics* **6** 106-124.
- RABINER, L. R. (1989). A tutorial on hidden Markov models and selected applications in speech recognition. *Proceedings of the IEEE* **77** 257-286.
- RAGHAVAN, V. (2016). Comparative analysis of activity profiles of different terrorist groups. *To be submitted for publication*.
- RAGHAVAN, V., GALSTYAN, A. and TARTAKOVSKY, A. G. (2013). Hidden Markov models for the activity profile of terrorist groups. *Annals of Applied Statistics* **7** 2402-2430.
- RDWTI, RAND Database of Worldwide Terrorism Incidents. Available: [Online].
<http://www.rand.org/nsrd/projects/terrorism-incidents.html>.
- SAGEMAN, M. (2004). *Understanding Terror Networks*. University of Pennsylvania Press.
- SANTOS, D. N. (2011). What constitutes terrorist network resiliency? *Small Wars Journal* **7**.
- TARTAKOVSKY, A. G., NIKIFOROV, I. V. and BASSEVILLE, M. (2014). *Sequential Analysis: Hypothesis Testing and Changepoint Detection*. CRC Press, Boca Raton, FL.
- TURGUT, S. (2007). Catalytic transformations for bipartite pure states. *Journal of Physics A: Mathematical and Theoretical* **40** 12185-12212.

ADDRESS OF FIRST AUTHOR
2 PETUNIA DRIVE, APT. 2H
NORTH BRUNSWICK, NJ 08902
E-MAIL: vasanthan_raghavan@ieee.org

ADDRESS OF SECOND AUTHOR
UNIVERSITY OF CONNECTICUT
STORRS, CT 06071
E-MAIL: alexg.tartakovsky@gmail.com